rept (NASA CR-54022)

OTS: $8.60 ph, $3.14 mf

1st QUARTERLY REPORT

RESEARCH AND DEVELOPMENT OF HIGH-PERFORMANCE LIGHT-WEIGHT FUEL CELL ELECTRODES

by

R. G. Haldeman, ~~Principal Investigator~~
W. A. Barber, and
W. P. Colman

prepared for

NATIONAL AERONAUTICS AND SPACE ADMINISTRATION

February 3, 1964 98 p refs

(NASA CONTRACT NAS 3-2786)

Period Covered: November 1, 1963 - January 31, 1964

NASA Lewis Research Center
Cleveland, Ohio
Space Power Systems Division
Technical Manager: Mr. W. A. Robertson MS-86-1

0171272

AMERICAN CYANAMID COMPANY
STAMFORD RESEARCH LABORATORIES
1937 West Main Street
Stamford, Connecticut
(Area Code 203) 348-7331

ABSTRACT

18162 A

The overall object of this contract is the reduction of the weight to power ratio of the hydrogen-oxygen fuel cell. Initial work has been concentrated on (1) materials studies including catalysts, supports and matrices, (2) modification of thin platinum/screen type electrodes, and (3) the development of evaluation procedures.

Catalyst studies included preparation of high area platinum blacks and evaluation of Pt-Rh-carbon systems. Studies of matrix materials indicated an asbestos-poly(vinyl alcohol) composition to show promise. Electrode variables included platinum loading, porosity, Teflon content and support screen structure. Design and operation of life testing equipment are described. Author

TABLE OF CONTENTS

TABLE OF CONTENTS

(Continued)

LIST OF TABLES

LIST OF FIGURES

1. INTRODUCTION

1.1 Objectives

The objectives of the National Aeronautics and Space Administration Contract NAS 3-2786 are indicated by Article I in the Statement of Work of RFP No. APGO-1508.

ARTICLE I - OBJECTIVES

(a) A fuel cell utilizing hydrogen and oxygen reactants is of considerable interest to NASA because of its high electrical work output per unit of weight of reactants. The efficiency of hydrogen-oxygen fuel cells is 60% or better in practical cells. These cells have a power plant weight of approximately 150 pounds per kilowatt neglecting reactants and tankage. The chief objective of hydrogen-oxygen fuel cell research is the reduction of the weight to power ratio.

(b) An important factor in determining the fuel cell weight is the weight of the electrode and its supporting structure. The intent is to support research and development efforts directed towards obtaining electrode systems which will produce a higher electrochemical reaction rate per unit weight of electrode and assembly while maintaining a satisfactory fuel consumption efficiency.

(c) While this RFP suggests that high-performance, light-weight electrodes are the basic interest, it should be understood that the weight and efficiency of the entire power plant must be included to in fact achieve the purpose of this effort; namely, the reduction of the fuel cell weight to power ratio.

1.2 Scope

The scope of work to be done by American Cyanamid Company is shown in the following outline which is a condensation of the Schedule of Work for Contract NAS 3-2786.

PHASE I

1. Materials Investigations

   Evaluation of available materials, as well as modification and development of new materials shall be carried out as required to permit choice of materials to be incorporated into components of high-performance hydrogen-oxygen fuel cells of improved power/weight ratio.

A. Catalysts

(1) Improvement of degree of uniformity and dispersion of platinum either as platinum black or as supported on a carbonaceous or fiber substrate.

(2) Study of synergistic effects of catalytic materials.

(3) Evaluation of nickel and/or cobalt borides and silver-containing catalysts at the anode and cathode of the alkaline cell, respectively.

(4) Investigation of catalyst substrate materials.

(5) Physical characterization of promising catalysts.

B. Supports

(1) Evaluation of wire and expanded metal screens of various dimensions for catalyst support and electrode matrix materials.

C. Matrices

(1) Evaluation of American Cyanamid Type B membrane.

(2) Evaluation of other matrix materials.

(3) Improvement of the characteristics of asbestos matrix material by modification of asbestos type and physical characteristics or by admixture of other fibers in the asbestos paper.

2. Electrodes

Available electrodes as defined below shall be evaluated, and modified electrodes fabricated and tested to the extent necessary to permit selection of candidates for extended testing.

A. American Cyanamid Type A Electrodes

Suitable screens containing a porous layer of platinum black and waterproofing agent spread uniformly and containing no extender.

B. American Cyanamid Type B Electrodes

Carbon-extended catalysts made into a paste and applied to suitable screens by techniques similar to those used for Type A electrodes.

C. American Cyanamid Type C Electrodes

Manufactured by paper-making techniques for the extension and uniform distribution of catalyst and waterproofing agent.

3. Performance Evaluation of Experimental Electrodes

Selected electrodes shall be tested for performance in suitable laboratory matrix type cells to provide service experience and design data for single cell prototypes of battery modules.

A. Initial performance in matrix type fuel cells, five square centimeters active area, will be determined concurrently with work in Phase I, Section 2 (Electrodes).

(1) Effect of cell structure and operating variables, significant for battery design.

B. Extended evaluation of promising electrodes in cells of 2" x 2" active area.

(1) Determination of physical characteristics of electrodes.

(2) A minimum of five cells will be operated at battery design loads for 100 hours of operation to study the effect of operating variables.

PHASE II

1. Single Cell Evaluation

Development of test of single cells as prototypes of ultimate battery structures.

A. Development of Cell with:

(1) Electrolyte matrix and electrodes of approximately battery dimensions.

(2) For a single preferred design as agreed upon by the NASA technical representative and American Cyanamid, conduct and analyze experiments to determine heat transfer, mass transfer and pressure drop of the fuel cell.

(3) Propose configuration and operating conditions which will maximize power/weight ratio for the system.

(4) Determine operational stability of the cell.

(5) Make a preliminary control system analysis.

2. Design Recommendations

Based on above developments, make preliminary design of a fuel cell battery having a weight to power ratio substantially lower than those presently available.

2. SUMMARY

Work in the initial quarter of the contract has been undertaken primarily under Phase I of the above schedule. Emphasis has been given particularly to (1) materials studies including catalysts, supports, and matrices, (2) study of modifications of American Cyanamid Type A and Type B electrodes, and (3) the development of suitable test vehicles for evaluation of both initial and life performance of the above electrodes. Considerable progress has been made in each area. Plans for work in second quarter of this contract are included in the last section of this report. Following is a summary of the major findings of the first quarterly report period.

1. Unusually high surface area platinum blacks were prepared by reduction of chloroplatinic acid with aromatic substituted silanes. These blacks, having specific areas of 40-60 m^2/g tend to be pyrophoric and sinter readily. Performance to date has not exceeded commercial blacks.

2. Platinum and rhodium codeposited on carbon were shown to operate synergistically when used as an anode electrocatalyst in the base cell. Initial performance at low loadings was equivalent to standard American Cyanamid Type AB-1 electrodes.

3. Matrix materials for the alkaline cell were investigated. Studies were made of various grades of commercially available asbestos paper, a specially prepared asbestos-poly(vinyl alcohol) matrix, and glass paper. The relation between resistivity and thickness was established. In general, more open structures were shown to favor lower resistivity, and the asbestos-poly(vinyl alcohol) paper showed considerable promise in this respect.

4. Modifications were made of American Cyanamid Company Type AB-1 electrodes by changing platinum loading, porosity, Teflon content, and support screen structure. Performance was analyzed statistically. Increased platinum loading produced a small but apparently significant improvement in performance. At the higher platinum loadings, lower Teflon level and more open screen structures were found to favor improved performance.

5. A theoretical analysis was made of the performance parameters of a matrix fuel cell in which water is removed by excess gas flow. Three conditions of feed gas were considered: dry gas, presaturated gas, and recirculated gas. It was found that if the cell is operated in the range 70-100°C and saturation is carried out at 20-25°C below cell temperature, and if a reasonable range of control of temperatures, external load and flow rates is assumed, electrolyte concentration can be held within ± 2N (± 5%) of initial concentration.

6. Cell performance at 70°C under conditions of water balance should virtually be independent of electrolyte concentration between 3 and 13N.

7. Design and operation of fuel cells having either one-inch diameter or 2 x 2 inch active area are described. These cells are suitable for both initial performance and life tests in the temperature range ambient to 100°C.

8. Initial life performance studies were made in 2 x 2 inch cells at 70°C using standard Type AB-1 electrodes. Most of the studies were made to explore operating conditions, e.g., relative gas flow rates and matrix compositions. It was found that using dry feed gases, longitudinal concentration gradients can develop in the matrix. Minimum gradients were obtained when the ratio of exit H_2 to exit O_2 was 1:2.

Up to 700 hours of relatively stable performance was observed although there were a number of occasions when control of the cell was lost. In general, electrodes removed from cells after life testing were found to retain their initial activities.

3. MATERIALS INVESTIGATION

3.1 Catalysts

Among the factors influencing the performance of fuel cell electrodes, the catalyst itself is of major importance. The catalyst must have as high as possible electrochemical activity for the reactant system under study or maximum performance will not be obtained. It is therefore, reasonable to assume that increased performance (i.e., higher sustained currents at a given voltage) can be achieved by increasing the number of electrochemically active sites on the catalyst. This might be done by increasing the surface area of the catalyst metal. Another approach might be to change the catalyst metal or to use a co-catalyst where a different (enhanced) electrochemical activity might be expected. Previous work indicated that these two directions showed promise. Both approaches have been followed during this report period and are discussed below.

3.1.1 High Area Platinum

Normal commercial platinum blacks have a surface area of roughly 20-30 m^2/g and a platinum crystallite size of 90 to 110 Å. American Cyanamid Company Type AB-1 electrodes are made from selected grades of commercial black. These electrodes, which have a loading of 9 mg/cm^2 platinum, are referred to in this report as "standard" electrodes. Our initial approach has been to make and test various samples of platinum black of surface area significantly greater than 30 m^2/g and in so doing to look for performance better than that obtained with standard Type AB-1 electrodes.

3.1.1.1 Preparation

Previous work has indicated that the nature of the reducing agent, the solvent, and the temperature all have an effect on the surface area of the resulting platinum black. In much of our previous work the room temperature reduction of chloroplatinic acid by sodium borohydride was used to produce catalysts. This method has been used extensively in the preparation of hydrogenation catalysts[1,2,3]. It is more reproducible than earlier reported reductions of platinum or other metals using formaldehyde[4] and hydrazine[5]. It has recently been reported[6] that substituted silanes give an active platinum catalyst for hydrogenation. It was indicated in a few of our early experiments that a modification of the reported silane reduction with subsequent isolation of the solid platinum black resulted in a very high surface area material. One very small sample of impure material had a measured surface area of 113 m^2/g, very high for an unsupported platinum black. Work during this report period has thus been concentrated on preparation of higher area platinum blacks by modification of sodium borohydride reduction and silane reduction.

All reductions were made in open glass containers with glass or Teflon stirrer blades or bars. Most samples of platinum black were made initially on a 2-gram scale. Five grams of chloroplatinic acid, for example, were dissolved in about 200 ml water and 40 ml of an approximately 5% solution of sodium borohydride added dropwise with constant rapid stirring. The sample was brought to a boil, cooled, filtered, washed free of chloride and dried in a vacuum desiccator to give about two grams of a fluffy platinum black.

In the case of silane reductions, the chloroplatinic acid was dissolved in ethanol (95%) at 75°C at the same concentration as above and the requisite silane (two moles per mole of chloroplatinic acid) dissolved in warm 95% ethanol. The warm silane solution was added slowly to the chloroplatinic acid to give a black solid which generally settled to the bottom of the beaker. The mixture was stirred for 30 minutes at 75°C, washed by decantation with hot alcohol and finally with water, then dried in a vacuum desiccator.

Caution must be used in exposing these active platinum blacks to air. If done too quickly, rapid heat evolution will cause the sample to sinter. It has been found adequate to pressurize the vacuum desiccator with nitrogen and then to allow slow equilibration with air by diffusion through the open stopcock. The tendency of these blacks to sinter complicates the interpretation of results of experiments in which they are used. A preliminary investigation of sintering is presented in Section 3.1.1.3.

Samples of prepared platinum blacks were characterized routinely by BET nitrogen surface area and platinum crystallite size by X-ray line broadening.

3.1.1.2 Evaluation

As a preliminary performance test, the platinum black powders were formed into an electrode containing 10 mg/cm^2 of platinum by mixing the black with Teflon added as a water emulsion (Teflon 30B - 60% solids) in an amount equal to 10% of the weight of platinum and Teflon and forming on a metal screen. The details of the method of preparation constitute proprietary information.

In testing for the catalyst program two one-inch circular electrodes were cut from the electrode sheet and assembled in a nickel metal cell (described in Section 5.2.2) with one filter paper soaked in 5N KOH as a matrix. Hydrogen was passed through both sides of the cell and an AC-resistance measurement made with a Universal Impendance Bridge. Measured cell resistances were in the range 0.06 ± 0.03 ohm. Oxygen was substituted for hydrogen on one side, the cell allowed to stand at open circuit for 10 minutes, and open circuit voltage measured on a Rubicon precision potentiometer. Current was drawn from the cell through a decade resistance and a DC polyranger Model S milliammeter (Sensitive Research Instrument Corp). At each current value chosen, the cell was allowed to operate for at least two minutes at steady potential before moving out to higher currents. The entire polarization curve out to 200 ma/cm^2 could be obtained in about thirty minutes. After the measurements were made at ambient temperature, the cell was heated to 70°C and another polarization curve taken. All results reported in this report are working voltages - no correction has been applied for internal resistance. The correction if applied would increase cell potential values at 200 ma/cm^2 by 60 ± 30 millivolts. These corrections are not of sufficient magnitude to influence the interpretation of the data.

A large number of catalyst preparations and preliminary performance tests with experimental materials on both sides of cell have been made and are reported in Table 3-1. Typical polarization curves are illustrated in Figures 3-1 to 3-6 which represent data taken at ambient temperature and 70°C.

TABLE 3-1

PROPERTIES OF EXPERIMENTAL PLATINUM BLACKS

Sample	Reducing Agent and Reduction Conditions	Surface Area m^2/g	Crystal Size Å	Preliminary Performance
Engelhard #8250	---	30	95	Very Good
Engelhard #7306	---	22	110	Fair-Good
183	$NaBH_4$ - H_2O - 0°C	12	110	Good
177	" " 25	13	100	"
184	" " 60	16	90	"
193	" " 80	12	105	"
178	" EtOH-H_2O 25	8	70	"
179	" Glycerol-H_2O 25	7	85	"
26	" H_2O 25 (Trace Pb)	12	110	"
37	" " 60 (rapid + dilute)	26	90	"
5	Hydrazine H_2O 25°C	0.6	110	Poor
16	Sodium formate H_2O 75°C	(ColloidalPt)		--
6	Triphenylsilane EtOH 75°C	61	40	Very Good
21	" " "	27	65	Good
25	" " "	8	70	Poor-Fair
23	Diphenylsilane " "	45	55	Good
49	" " "	42	70	Good
19	Tribenzylsilane " "	51	40	Fair-Good
55	Triethoxysilane " "	34	50	Good
24	Triethylsilane " "	18	55	Good
58	" " " (dilute)	>15		Fair-Good
32	" isopropanol "	26	70	Very Good
29	" Glyme "	5	70	Poor
56	Tri-n-butylsilane EtOH "	13	50	Good
61	" " " (dilute)	>15		Good

(1) Experimental blacks on both sides of cell.

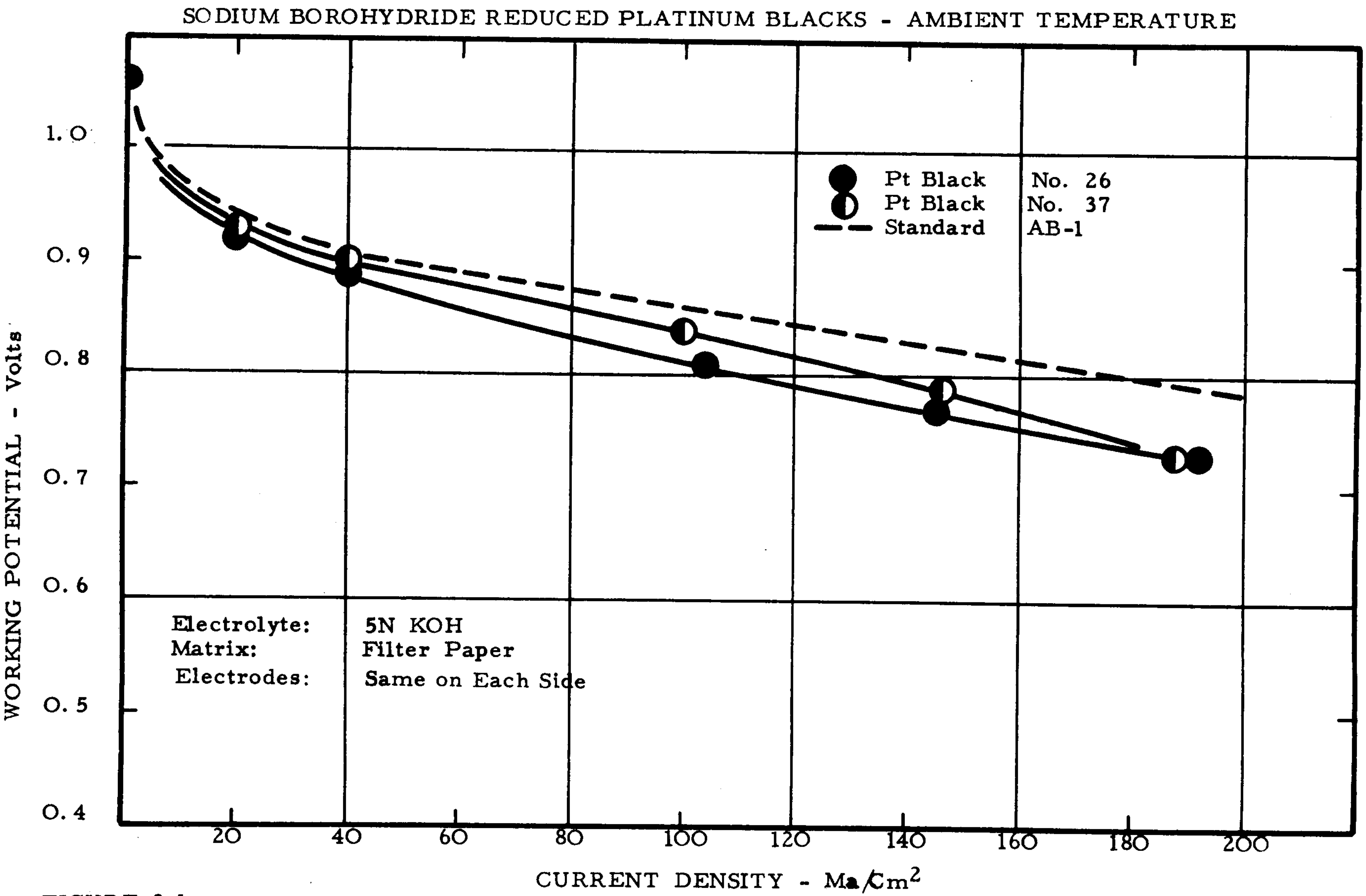
SODIUM BOROHYDRIDE REDUCED PLATINUM BLACKS - AMBIENT TEMPERATURE
Pt Black No. 26
Pt Black No. 37
Standard AB-1
Electrolyte: 5N KOH
Matrix: Filter Paper
Electrodes: Same on Each Side
1.0
0.9
0.8
0.7
0.6
0.5
0.4
WORKING POTENTIAL - Volts
20
40
60
80
100
120
140
160
180
200
CURRENT DENSITY - Ma/Cm2

FIGURE 3-1

SODIUM BOROHYDRIDE REDUCED PLATINUM BLACKS - 70°C

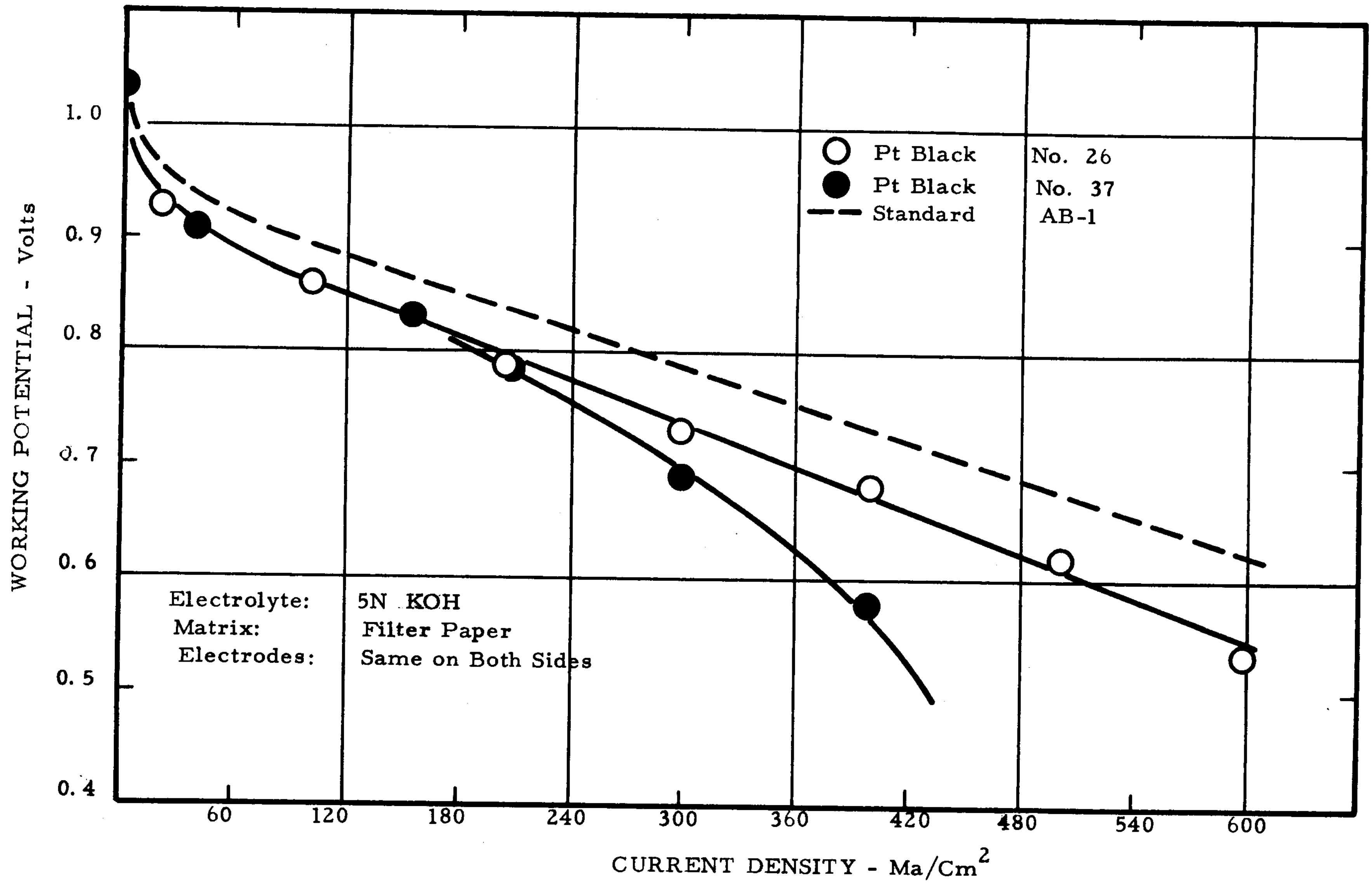

FIGURE 3-2

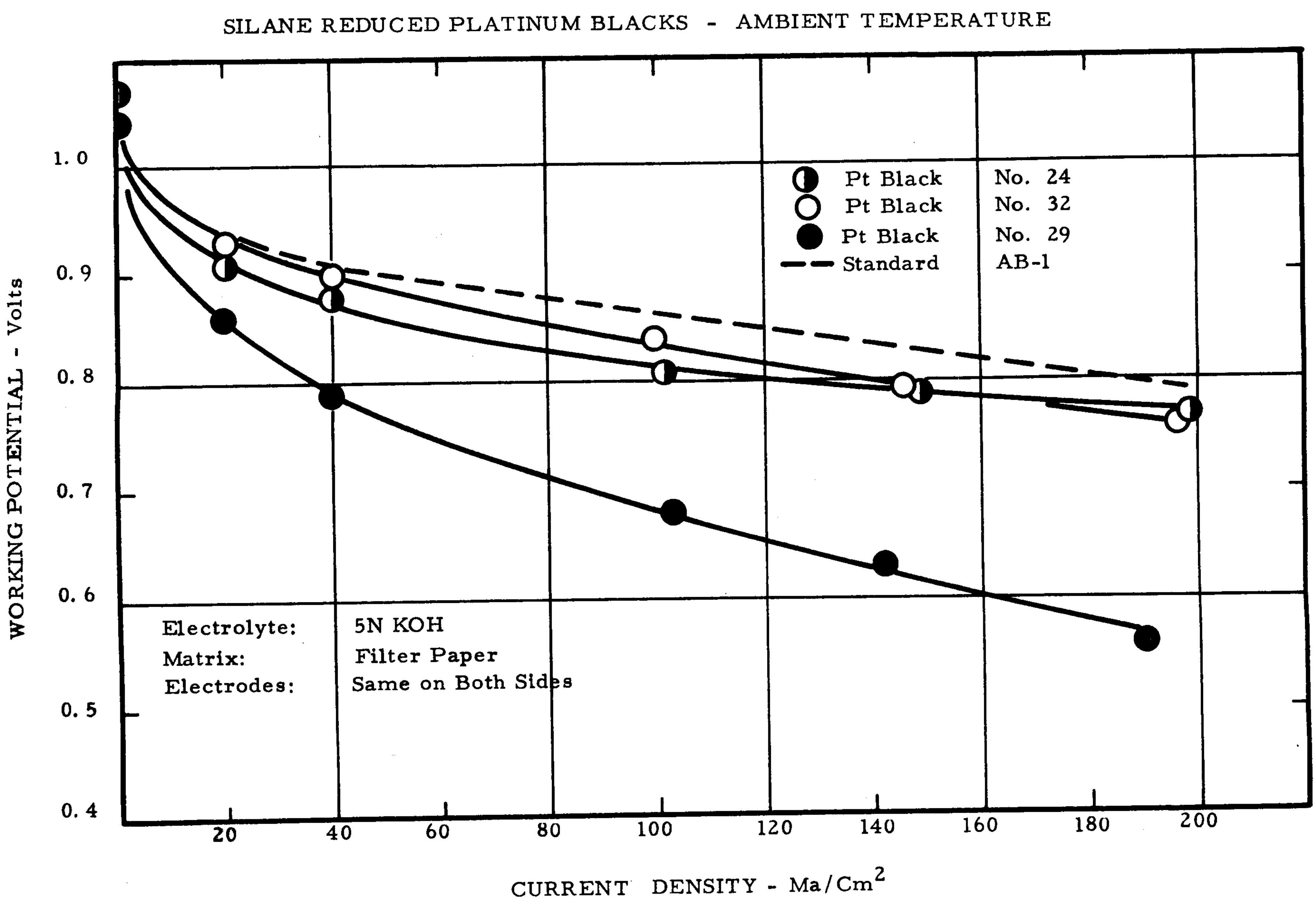
SILANE REDUCED PLATINUM BLACKS - AMBIENT TEMPERATURE
Pt Black No. 24
Pt Black No. 32
Pt Black No. 29
Standard AB-1
Electrolyte: 5N KOH
Matrix: Filter Paper
Electrodes: Same on Both Sides
WORKING POTENTIAL - Volts
1.0
0.9
0.8
0.7
0.6
0.5
0.4
20
40
60
80
100
120
140
160
180
200
CURRENT DENSITY - Ma/Cm²

FIGURE 3-3

SILANE REDUCED PLATINUM BLACKS - 70°C

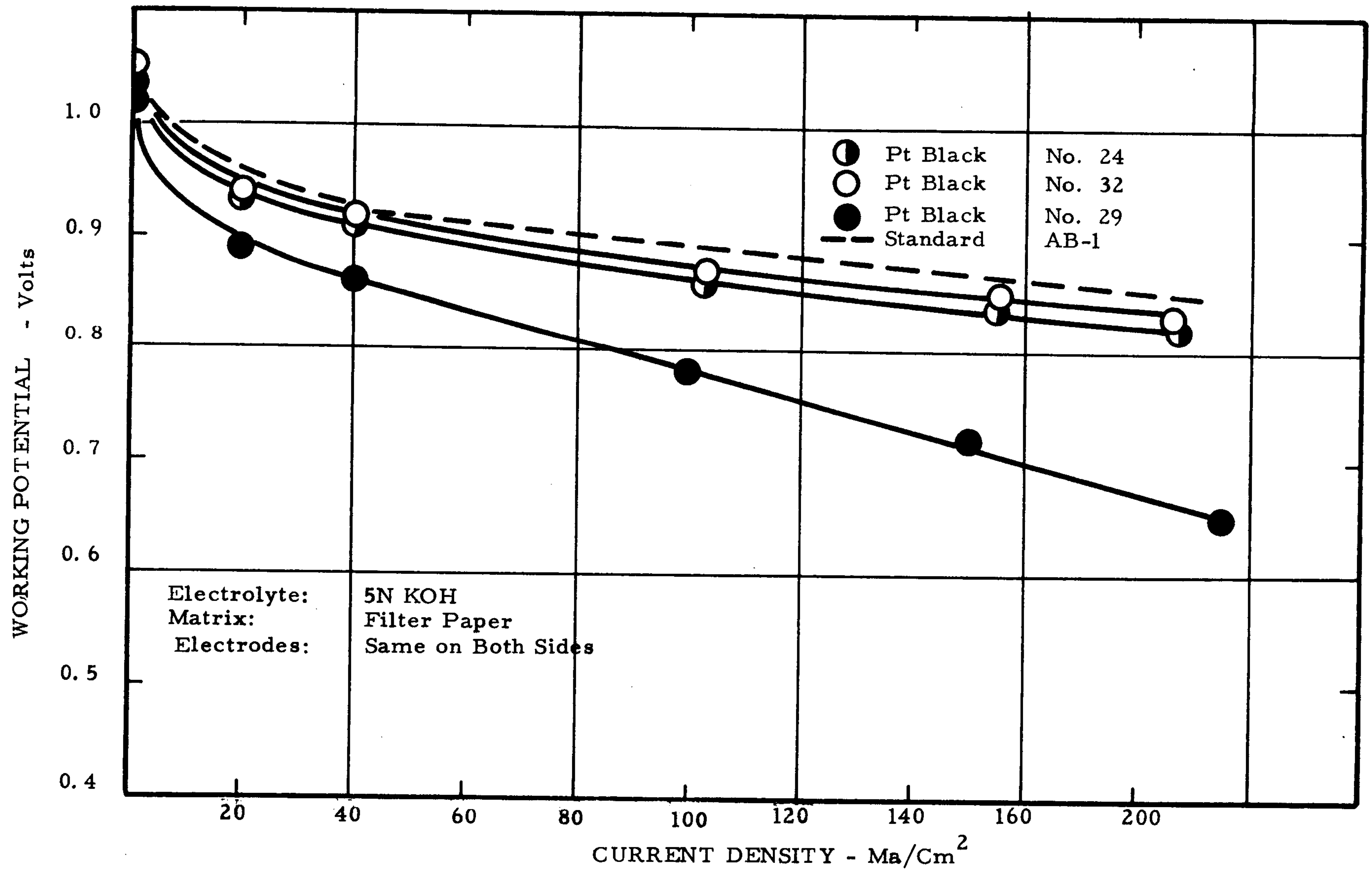

FIGURE 3-4

SILANE REDUCED PLATINUM BLACKS - AMBIENT TEMPERATURE

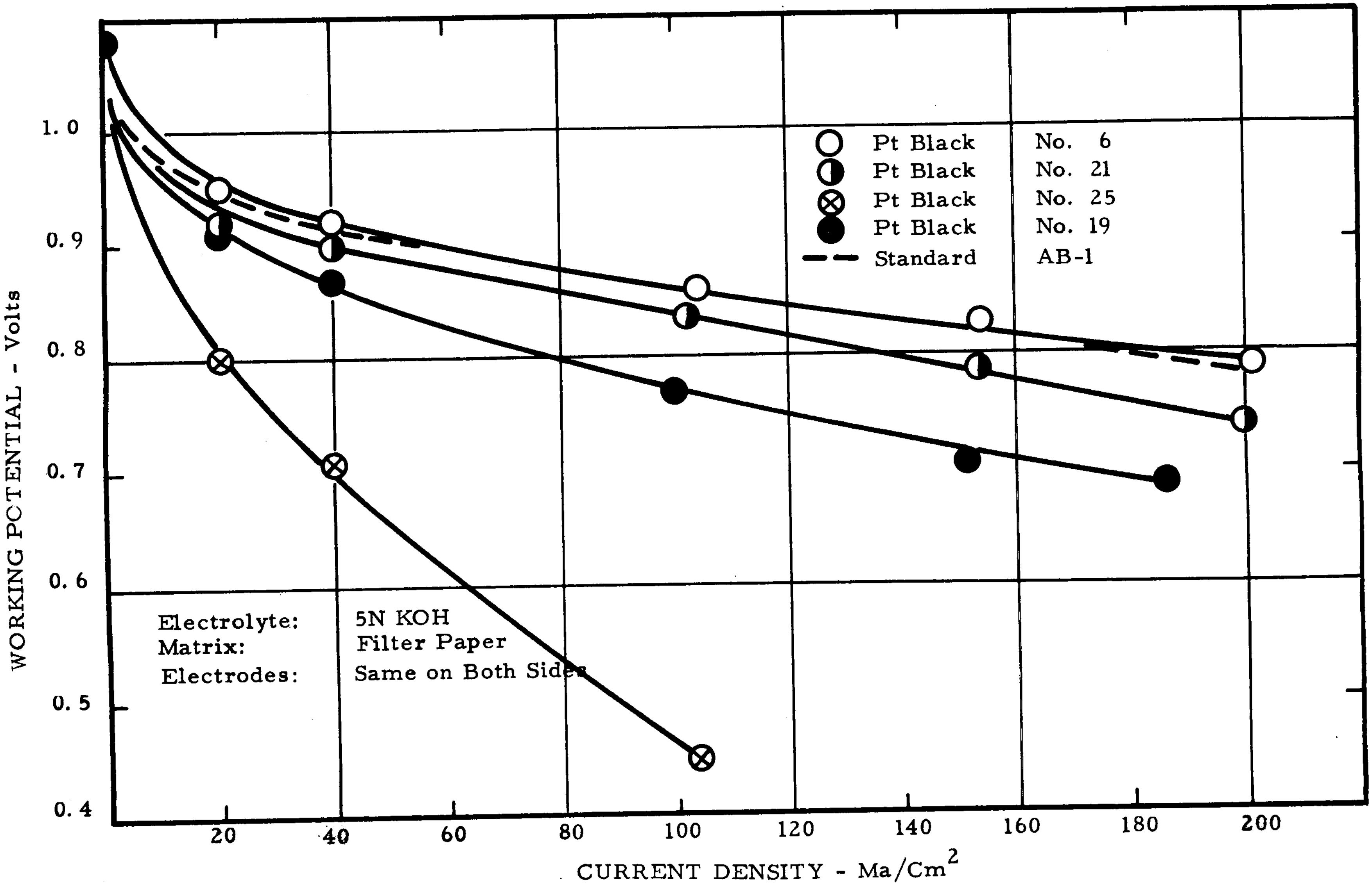

FIGURE 3-5

SILANE REDUCED PLATINUM BLACKS - 70°C

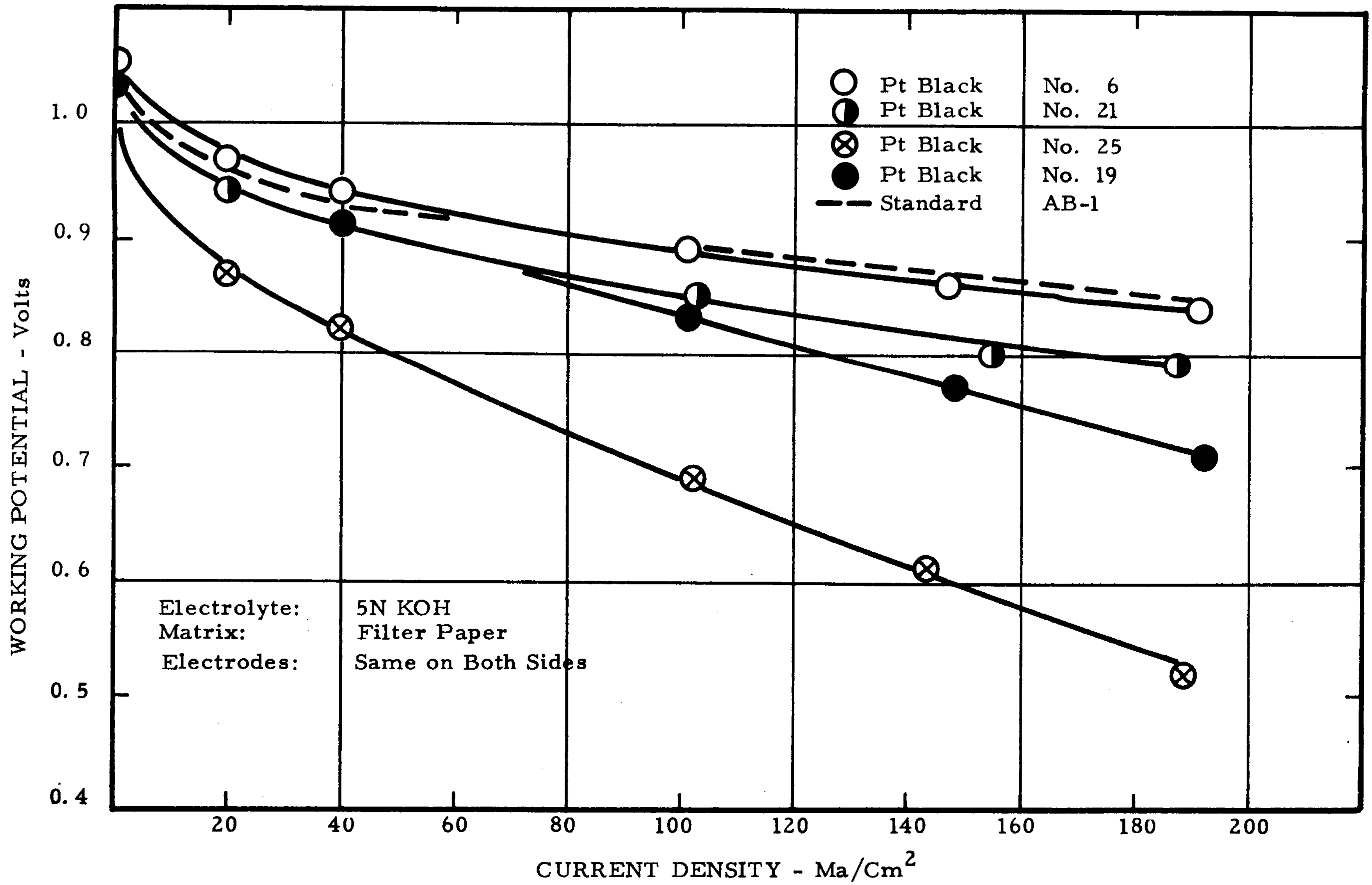

FIGURE 3-6

A number of conclusions can be reached tentatively from these data.

In a series of sodium borohydride-reduced platinum blacks varying in surface area from 7 m^2/g to 26 m^2/g and in crystal size from 70 Å to 110 Å, the best performance as shown in Figure 3-1 was not quite as good as the better grades of commercial platinum blacks. Highest area blacks made by borohydride reduction were obtained by rapid mixing of reactants in a water solution at 60°C, and this regime of conditions will be the subject of further investigation.

A few reductions with hydrazine (No. 5 in the table is typical) produced a mixture of bright and black platinum not catalytically active, while reductions with formaldehyde and formate solutions were irreproducible and in many cases resulted in either bright platinum mirror deposits or relatively stable colloidal platinum dispersions.

Reduction with a variety of substituted silanes in alcohols at 75°C gave some preparations with very high surface area and low crystallite size. Surface areas in the range of 40-60 m^2/g seem to be attainable with 2-5 gram preparations. One experiment (which produced Sample No. 26) with triethylsilane indicated a possible improvement could be obtained by using isopropanol instead of ethanol as a solvent. As indicated in Table 3-1, the aromatic substituted silanes tend to give higher surface area platinum blacks than do the aliphatic silanes.

Some typical polarization curves for silane-reduced samples are shown in Figures 3-3 to 3-6 inclusive. Performance of the silane-reduced platinum blacks ranged from poor to very good. However, when formed into electrodes in our usual way and used in our standard test procedure, they failed to show a significant improvement in performance over standard blacks.

The preceding section of work was essentially a screening program. Two of the high area platinum samples (Nos. 23 and 49 prepared by diphenylsilane reduction, giving surface areas of 45 and 42 m^2/g, respectively) were selected for more detailed study and comparison with commercial platinum black. In addition, samples were tested having surface areas of only 5 and 3 m^2/g produced by sintering high area blacks during H_2 treatment (see 3.1.1.3).

Electrodes were prepared from these blacks on 100-mesh Ni screen with varying amounts of Teflon. High and low surface area materials were evaluated at ambient temperature on the O_2 side of a base cell vs. standard electrodes on the hydrogen side. High surface area material was run also on the H_2 side of a base cell against a standard electrode on the oxygen side. These results are shown in Table 3-2.

The following observations and conclusions were drawn from this work:

1. Higher area blacks (42-45 m^2/g) in the present type of electrode formulation have shown little, if any, advantage over commercial blacks, although it is possible that optimum structures have not yet been made.

2. With higher area blacks the Teflon level appears to be fairly critical for optimum electrode performance. This is in contrast to electrodes, made from commercial blacks, in which Teflon level has not a very strong influence.

TABLE 3-2

EFFECT OF PLATINUM SURFACE AREA

ON PERFORMANCE RELATIVE TO STANDARD TYPE AB-1 COUNTER ELECTRODE

AMBIENT TEMPERATURE

Electrode Studied	Surface Area of Platinum, Electrode Studied m^2/g	Total Load mg/cm^2	Teflon %	Voltage at 40 ma/cm^2	Voltage at 180 ma/cm^2
O_2	30 (Commercial Black)	9	20	.925	.835
		10	20	.93	.83
		15	20	.935	.835
O_2	45	9	5	.85	-
			10	.87	.76
			20	.91	.85
			35	.86	.73
O_2	42	10	20	.915	.805
		15	20	.92	.82
O_2	5	9	20	.89	.80
	3	15	20	.86	.75
H_2	30 (Commercial Black)	10	20	.92	.82
H_2	45	10	10	.90	.78
			20	.88	.74

3. Increasing platinum loading from 9 or 10 to 15 mg/cm^2 has a relatively small effect on performance. (The effect of platinum loading in standard electrode formulations will be discussed in detail in a later section.)

4. The extent and effect of sintering of platinum in the formed electrodes should be investigated. A start in this direction is discussed in the next section. As may be seen from Table 3-2, electrodes prepared from highly sintered blacks performed nearly as well as the higher area blacks.

3.1.1.3 Sintering

It was noted in handling some of the high area blacks prepared in the course of this work that some preparations were pyrophoric and required special handling. In particular, exposure of a freshly reduced dry sample to air caused considerable evolution of heat. A gradual exposure to air is now always used to minimize any heating effect. It was (and still is) a pertinent question whether the surface area of the sample changed with handling or with exposure to a reactive gaseous atmosphere.

A decrease of surface area on hydrogen treatment was observed for both a laboratory sample and a commercial platinum black by enclosing the powdered sample in a tube on a vacuum line and alternately measuring the BET nitrogen surface area and exposing the sample to hydrogen at low temperature (starting at -196°C) without intermediate exposure to air. A steady decrease in surface area from 30 to 10 m^2/g was observed in two hydrogen treatments of the commercial sample. The laboratory sample was reduced in surface area by the same treatment from 40 to 7.5 m^2/g which suggests a greater sintering effect for the laboratory sample.

Also, a fact which is very interesting, although the measured nitrogen surface area for the laboratory sample was higher initially than the commercial sample, the amount of hydrogen adsorbed per unit weight was smaller. This is not expected and needs more work to clarify. It could be explained by differences in the exposed platinum crystal faces on the two samples or differences in "solubility" of hydrogen in the platinum.

That loss of surface area needs to be considered as a factor in our work can be seen from Table 3-3. It lists surface areas measured before and after treating degassed air-exposed platinum black samples with hydrogen at ambient temperature.

This sintering effect has been noted earlier (with different treatments) by several investigators[7,8,9,10,11] although McKee[8,9] implies that it takes place only above 100°C.

A few experiments have been run to see if the surface area changes on hydrogen treatment of a standard platinum black after it has been formed into an electrode on a heat-conducting screen. Results indicate that about one-third of the original surface area of the black was covered up in making each of the two electrodes tested. Also there was a relatively small but significant decrease of surface area (10%) on exposure of the electrode to hydrogen treatment. It is not known yet whether this decrease continues on repeated alternate exposure to oxygen and hydrogen. If so, it could account for losses in performance observed when electrodes are repeatedly assembled and disassembled in a cell.

The stabilizing effect of the support screen may be a very important factor in maintaining high electrode activity. Similar measurements will be made on the high area blacks.

TABLE 3—3

AMBIENT TEMPERATURE SINTERING OF PLATINUM BLACKS

Sample	As Made: Surface Area m^2/g	As Made: Crystal Size Å	H_2-Treated at Ambient Temp.: Surface Area m^2/g	H_2-Treated at Ambient Temp.: Crystal Size Å
19	51	40	9	80
19	44	--	3	--
21	27	65	4	> 200
21	25	--	5.5	--
23	45	55	2	> 200
23	43	--	4.6	--
24	18	55	4	170
24	18	--	5	--
25	7	--	3	--
26	10	--	7	--
27	9	--	6	--
Commercial	33	90	9	120

3.1.2 Platinum-Rhodium-Carbon

In catalyst research synergistic effects of catalytic materials have frequently been found. In particular, combinations of platinum with other metals have been shown to improve performance or reduce usage of expensive ingredients[13,14]. Some work with platinum-rhodium mixtures as hydrogenation catalysts has recently been reported[12]. Our work shows the latter system has promise for fuel cell anodes in the base system, particularly at low catalyst loadings.

3.1.2.1 Preparation

The catalysts studied in this work were either platinum or rhodium blacks prepared by sodium borohydride reduction as described in Section 3.1.1.1 or were deposited on any of several powdered carbon supports. To prepare a supported catalyst, a weighed amount of carbon was slurried in aqueous suspension and to the slurry was added the proper amount of chloroplatinic acid, rhodium chloride, or a mixture of the two in the desired proportion. Enough 5% sodium borohydride solution was added dropwise to reduce the metals (see Section 3.1.1.1) and the resulting metallized carbon was heated to boiling, cooled, filtered, washed free of chlorides and dried in a vacuum desiccator. When both rhodium chloride and chloroplatinic acid were reduced simultaneously, a co-deposited catalyst was obtained. Electrodes were prepared from these catalysts by a proprietary process and fall within the category designated as American Cyanamid Company Type B electrodes.

3.1.2.2 Evaluation

In view of the finding in prior investigations of a synergistic effect at low loadings of Pt and Rh, work for this contract was directed toward the use of Pt/Rh combinations supported on carbons at higher loadings to determine if further improvements in anode performance could be made. A survey was made of the following variables of composition: total loading, Pt/Rh loading, and Teflon content. The carbon support chosen for this work was Stackpole C-2H flour, which gave satisfactory performance and had convenient properties in electrode manufacture. Polarization data for cells consisting of experimental hydrogen electrodes and standard oxygen electrodes are shown in Table 3-4. Since our earlier work at low concentrations of Pt/Rh indicated optimum weight ratio of these two metals to be near unity, this ratio was used for nearly all mixtures.

The synergistic effect of Pt/Rh found in our earlier work at low loadings (1.0 mg total) is clearly shown in the last three lines of the table. The synergistic effect relative to platinum alone at the same total loading of noble metal seems to diminish as loading is increased, so that performance becomes as good but not better than a standard Type AB-1 electrode at a loading of 9 mg Pt/cm^2. In fact, at least in this initial performance test, all Pt/Rh electrodes having ratio of noble metals of unity perform as well as the standard within about 30 mv at currents of 40 and 180 ma/cm^2. The range of the data is shown in Figure 3-7.

It is interesting, also, that both total loading of material on the electrode (over the range of 10 to 40 mg/cm^2) and level of Teflon (10 to 20%) have no significant effect on performance.

TABLE 3-4

PERFORMANCE OF PLATINUM/RHODIUM ELECTRODES; H_2 SIDE OF BASE CELL

AMBIENT TEMPERATURE

Rhodium mg/cm²	Platinum mg/cm²	Carbon mg/cm²	Total Load mg/cm²	Teflon %	Voltage at 40 ma/cm²	Voltage at 180 ma/cm²
0.0	9.0	0.0	9.0	20	.88	.80
2.5	7.5	0.0	10.0	20	.87	.77
5.0	5.0	10.0	20.0	20	.88	.80
5.0	5.0	10.0	20.0	10	.88	.77
2.5	2.5	15.0	20.0	20	.90	.80
2.5	2.5	15.0	20.0	10	.88	.80
2.5	2.5	5.0	10.0	20	.89	.80
-	5.0	15.0	20.0	20	.86	.75
2.0	2.0	36.0	40.0	10	.90	.77
1.0	1.0	18.0	20.0	10	.90	.80
1.0	1.0	18.0	20.0	20	.88	.78
1.0	1.0	8.0	10.0	10	.87	.77
-	2.0	18.0	20.0	20	.85	.68
0.5	0.5	19.0	20.0	10	.90	.79
1.0	0.0	19.0	20.0	10	.85	.73
0.0	1.0	19.0	20.0	10	.83	.68

RANGE OF PERFORMANCE PLATINUM-RHODIUM-CARBON ELECTRODES

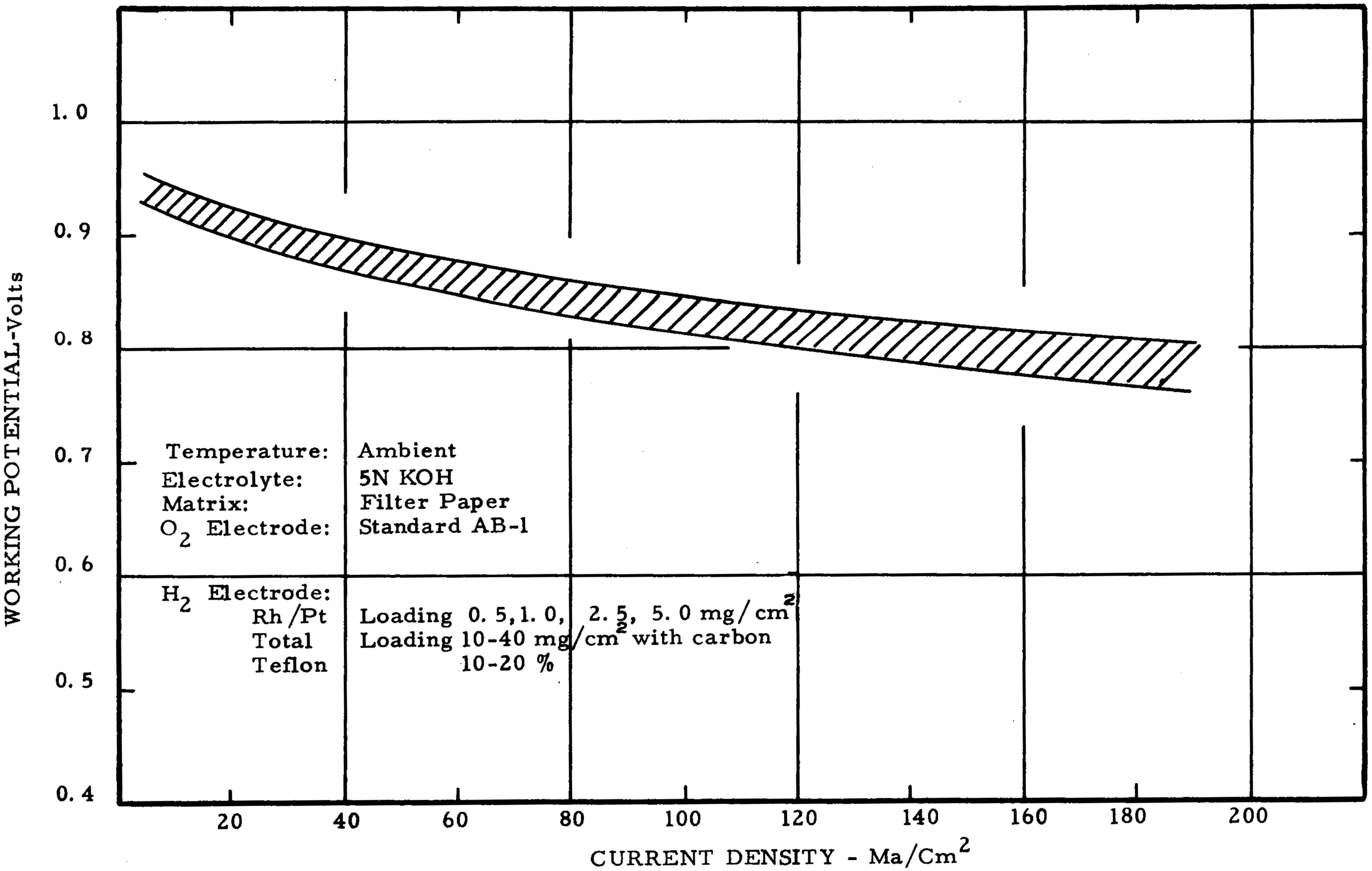

FIGURE 3-7

We conclude from this work based on initial polarization data only, that it is unlikely that marked improvements in anode electrocatalysts can be made over platinum as found in our standard Type AB-1 electrodes. Rather, further improvements in cell performance will probably come from improvements in cathode electrocatalysts, optimization of cell structure, and optimization of cell operating conditions. These topics furnish the basis for further work in the development of thin, light-weight, high-performance fuel cell electrode systems. On the other hand, Pt/Rh catalyst mixtures at low loading show considerable promise of reducing usage of noble metal.

3.2 Matrices

To be suitable for use in alkaline fuel cells, the matrix material must be chemically stable in hot KOH solutions. It should offer minimum resistance to hydroxyl ion transport, and should be hydrophilic in order to permit rapid equilibration of water. Various types of asbestos appear to satisfy these general criteria. In order to aid in the selection of a standard matrix material for use in life tests, a study has been made of physical characteristics and fuel cell performance for a number of available materials. The initial objective of this work was to compare various forms of asbestos with filter paper, which has been used extensively in electrode evaluation work to date.

3.2.1 Materials Studied

Matrix materials studied in this phase of the program are listed in Table 3-5.

TABLE 3-5

MATRIX MATERIALS

Material	Source
Whatman #42 Filter Paper	A. H. Thomas
Fuel Cell Asbestos Board, 30 mil and 10 mil grades	Johns-Manville
#10 Quinterra Asbestos	Johns-Manville
"ACCO" Asbestos	Internal
Whatman GF/B Glass Fiber Paper	A. H. Thomas

Mineralogical examination shows that the Johns-Manville asbestos samples are both of the mineral form chrysotile, ($Mg_6(OH)_8Si_4O_{10}$), but differ in the type and amount of impurities present. The Fuel Cell Asbestos Board is an Arizona chrysotile, and contains an estimated 2-4% of carbonate minerals such as calcite ($CaCO_3$) and dolomite $[CaMg(CO_3)_2]$. The Quinterra asbestos is a "de-ironed" Canadian chrysotile, containing very low carbonate impurity (probably less than 0.5%), but with traces of chromite ($FeCr_2O_4$). Analysis of the Quinterra paper showed 1.97% Fe, as compared with 0.34% Fe for the Fuel Cell Asbestos Board. The 30-mil thick Asbestos Board is a composite sheet consisting of approximately twelve two-ply sheets pressed together.

The "ACCO" asbestos sheet is an experimental material made from a caustic-leached tremolite $[Ca_2Mg_5Si_8O_{22}(OH)_2]$ asbestos, with 10% polyvinyl alcohol fiber as a binder. Starting materials are Baker & Adamson Acid-Washed Long-Fiber Asbestos (Code No. 1393), and Kuralon® PVA fiber, obtained from the Kurashiki Rayon Co., Ltd., Japan.

The asbestos fiber was given three successive leaches (4-6 hours each) with 25% KOH at 90-100°C before being made into a sheet with the PVA fiber binder. In the first leach, an amount of silica equivalent to approximately 1-2% of the original asbestos weight was extracted. No significant amount of material was extracted in the subsequent leaches. Similar treatment of the two Johns-Manville asbestos papers showed no significant amount of material extracted.

Glass-fiber is not stable in hot KOH and would not be suitable for use in an alkaline fuel cell. It was included in this study because it is an example of a material with an extremely open physical structure.

3.2.2 Polarization Data - Matrix Materials

Polarization data were obtained on the various asbestos materials described in Section 3.2.1, using standard American Cyanamid Type AB-1 electrodes in 1" test cells. The tests were run at 70°C, with hydrogen and oxygen, and 5N KOH electrolyte. The data are summarized in Table 3-6. Cell performance with the as received nominal 30-mil Fuel Cell Asbestos Board was somewhat low. In thinner sections, however, performance comparable with that for the other materials tested was obtained.

3.2.3 Resistivity Measurements

The electrical resistance offered by an electrolyte-saturated matrix is an important factor in fuel cell performance. Electrical resistance would be expected to depend on the physical structure of the matrix. In particular, the porosity of the matrix should be important.

TABLE 3-6

POLARIZATION DATA: MATRIX MATERIALS

	Fuel Cell Asbestos Board			#10 Quinterra	"ACCO" Asbestos	Filter Paper[2] (#42 Whatman)
Thickness, mils (Dry, uncompressed)	37[3]	20	14	10	25	10
Current Density: (ma/cm^2)	Working Voltage[1]					
0	1.044	1.044	1.040	1.025	1.06	1.036
40	0.903	0.917	0.913	0.916	0.935	0.923
100	0.845	0.879	0.901	0.836	0.898	0.884
200	0.749	0.834	0.852	0.848	0.846	0.844
300	0.668	0.784	0.817	0.817	0.793	0.812
400	----	0.735	0.773	0.781	0.740	0.769

(1) At 70°C, 1" Hydrogen-oxygen cell, 5N KOH electrolyte. Type AB-1 electrodes.

(2) Average of three tests.

(3) Nominal 30 mil thickness. The thinner sections were obtained by delaminating the "as received" material.

Since the materials of interest are generally compressible, porosity will be a function of the pressure applied to the matrix. In order to help characterize the various matrix materials listed in Section 3.2.1, independent measurements were made of thickness and electrical resistivity as a function of applied pressure. From these measurements, a comparison of the electrical resistance of the materials at the same thickness can be made.

Matrix thickness as a function of pressure was determined by placing one or more 3" x 3" layers of the electrolyte-saturated material between two standard fuel cell endplates. Thickness of the entire assembly was measured with an Ames Comparator, previously zeroed for the thickness of the end-plates alone. The four bolts of the assembly were then tightened to 5, 10, and 15 inch-lbs. torque, and the thickness noted at each level. Pressure on the sample was calculated from the relationship:

$$P = \frac{n\,T}{0.2\,dA}$$

where: P = pressure, lbs/in^2

T = applied torque, in-lbs.

A = sample area, in^2

d = major diameter of bolt, inches

n = number of bolts

An estimate of the porosity of the material at a given pressure can be made by calculating density from the weight of the dry sheet and its compressed thickness, and then applying the relationship:

$$V_o = 100\,(1 - \rho/\rho_o), \text{ where}$$

V_o = Void volume, %

ρ = Bulk density, as measured

ρ_o = Skeletal density for the matrix material

Figure 3-8 shows characteristic thickness vs. applied pressure curves for the various materials tested. Calculated void volumes vs. applied pressure are shown in Table 3-7. All of the materials were compressed to about one half of their original dry thickness at 120-180 psi. This is the approximate compressive load normally applied in a 2" x 2" test cell. All of the materials except the "ACCO" asbestos and the glass fiber paper swelled to approximately 150% of their dry thickness when saturated with electrolyte. The binder added to the "ACCO" asbestos prevents swelling, and provides an appreciable degree of wet-strength to the paper.

The resistance of the matrix saturated with 5N KOH was determined in a standard 1" cell (see Section 5.2.2 for details) using a full 3" x 3" sheet of the matrix material. For each material, overall cell resistance at room temperature was measured over a range of applied pressure, and for varying numbers of sheets. The relationship between cell resistance and pressure is indicated by the curves in Figure 3-9.

MATRIX THICKNESS VS. PRESSURE

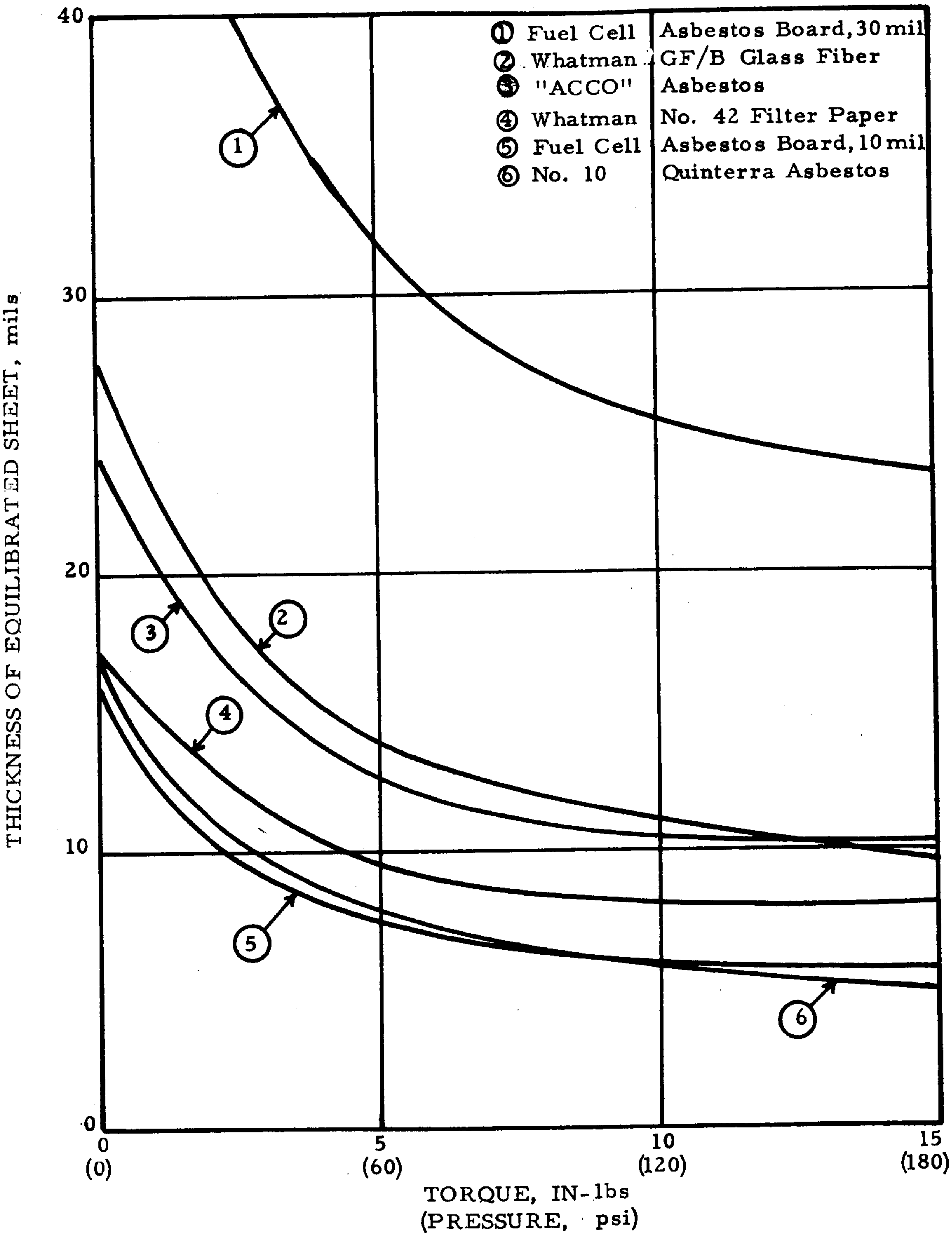

FIGURE 3-8

TABLE 3-7

CALCULATED VOID VOLUMES[1] VS. PRESSURE

Pressure, psi		0	60	120	180
Material	Skeletal Density (g/cc)	Void Volume, %			
Whatman GF/B Glass Fiber	2.5	94	83	79	75
"ACCO" Asbestos	3.0	88	78	74	73
Whatman #42 Filter Paper	1.4	74	72	67	63
#10 Quinterra Asbestos	2.5	78	71	60	55
Fuel Cell Asbestos, 30 mil	2.5	68	63	53	49
Fuel Cell Asbestos, 10 mil	2.5	69	59	50	45

(1) Values at 0 psi calculated from dry thickness measurements. Values at other pressures calculated from thickness of electrolyte-saturated matrix.

CELL RESISTANCE VS PRESSURE

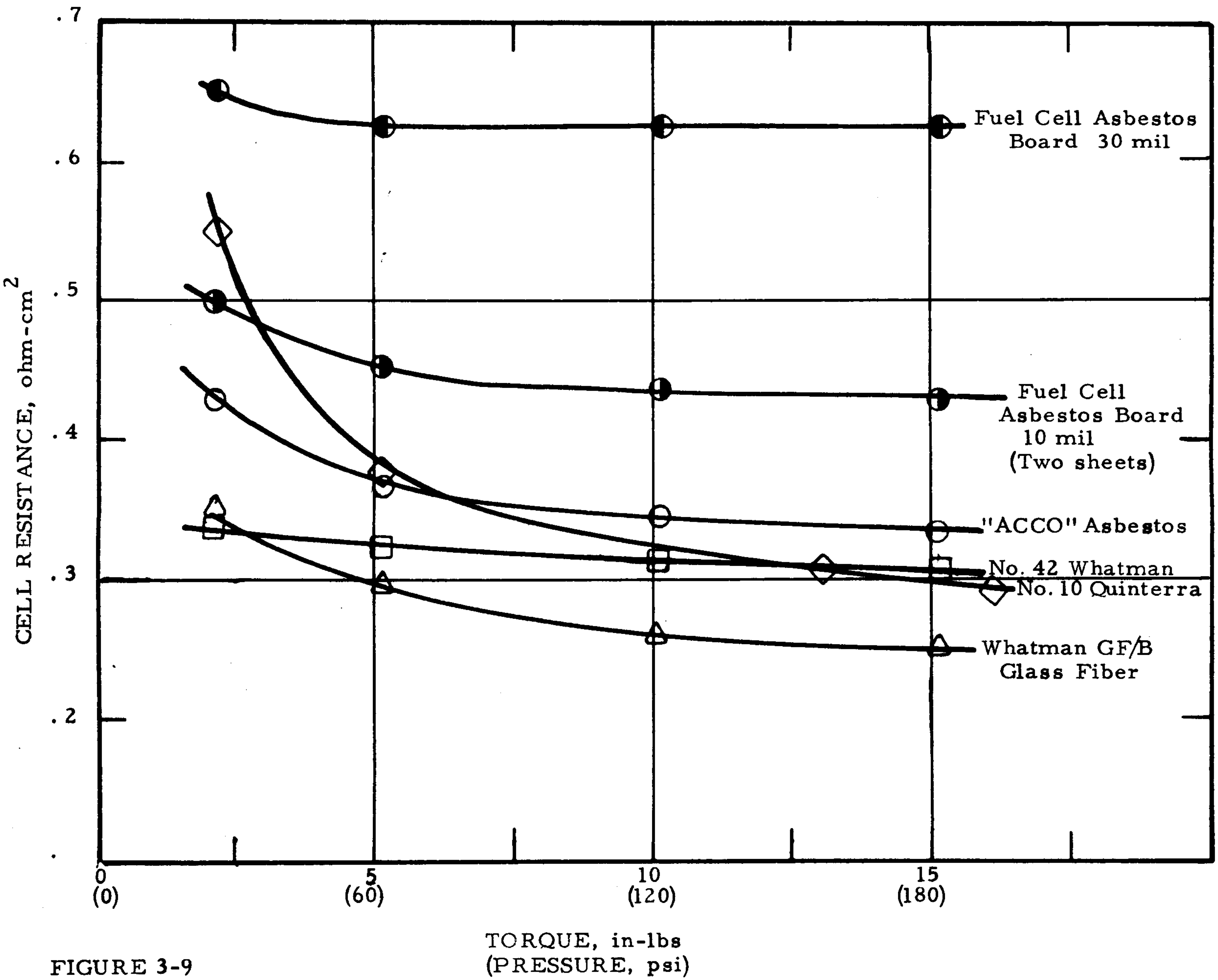

FIGURE 3-9

By combining the data from the thickness and resistance measurements, a plot can be made of cell resistance vs. compressed matrix thickness for a given applied pressure. The data at 15 in-lbs torque (180 psi) are shown in Figure 3-10. Note that for all materials, the relationship between resistance and thickness is linear, and that all materials have a common intercept at zero thickness. This intercept represents the sum of all components of cell resistance other than that for the electrolyte-saturated matrix; i.e., electrode, current collector, and contact resistances. From the slope of the line, the specific resistivity of the electrolyte-saturated matrix in its compressed state can be calculated. For the data in Figure 3-10, the specific resistivity at 180 psi ranges from 5.2 ohm-cm for the glass-fiber paper to 12 ohm-cm for the #42 paper. This is approximately three to eight times the resistivity of 5N KOH alone (1.6 ohm-cm)[15]. Note that the glass fiber paper and the "ACCO" asbestos, which have the greatest porosity (Table 3-7), also have the lowest resistance (Figure 3-10). For thin matrices, the differences in resistance indicated by this study would not have a major affect on performance. At a compressed thickness of 10 mils, for example, the greatest difference between the various forms of asbestos studied appears to be on the order of 0.1 ohm-cm^2, corresponding to a difference in voltage of 10 mv at a current density of 100 ma/cm^2. For thicker matrices, and particularly at higher current densities, the lower resistance of the "ACCO" asbestos would appear to offer an advantage over the commercial materials.

CELL RESISTANCE VS MATRIX THICKNESS

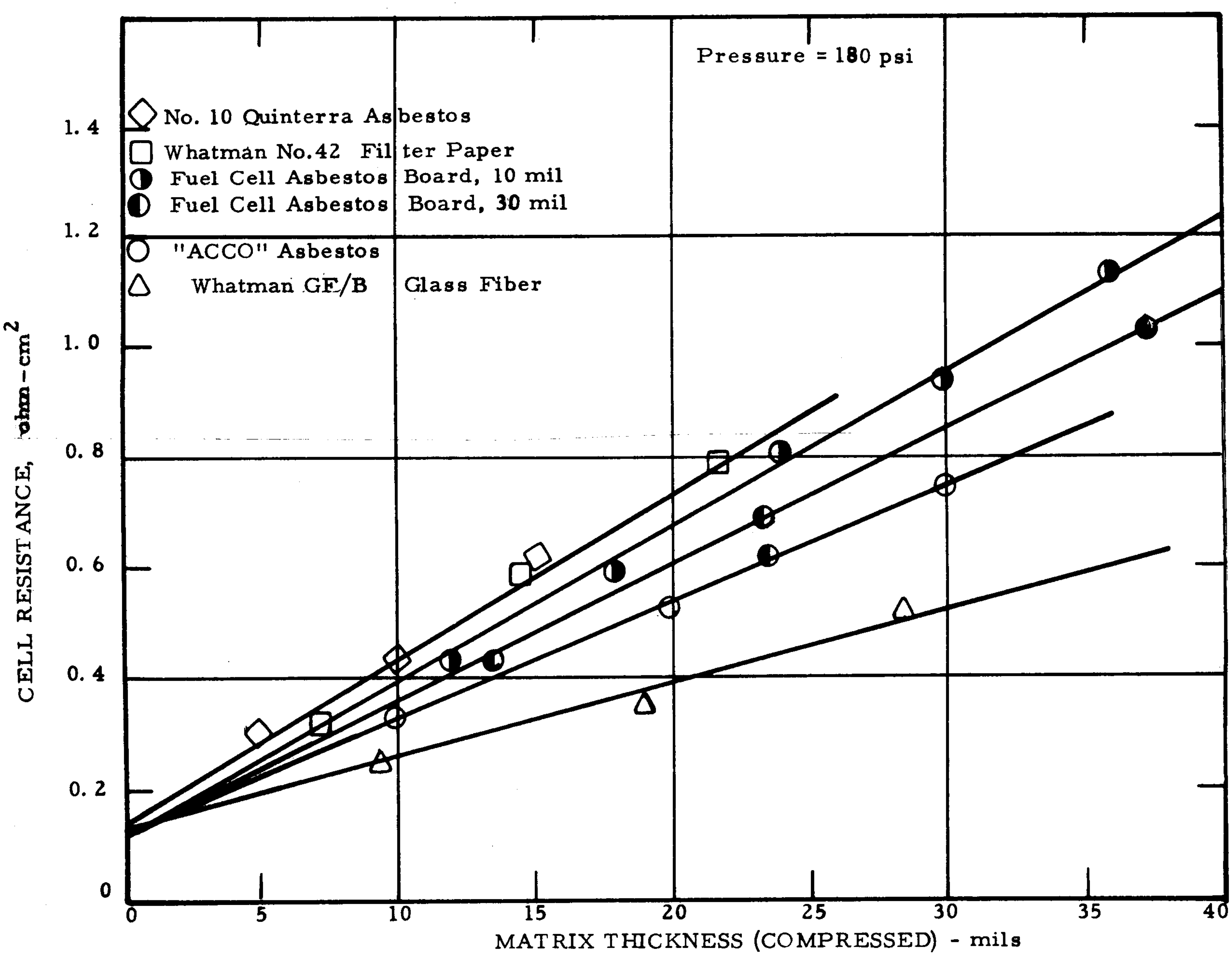

FIGURE 3-10

4. ELECTRODE DEVELOPMENT

One of the principal objectives of the work being done under this contract is to maximize performance in the base system. In earlier sections of this report, work directed toward achieving this objective through the use of new or modified catalyst materials has been discussed. The work reported in this section was directed toward obtaining maximum performance with standard platinum black, through modification in electrode composition and structure. The platinum black used in this work was obtained from Engelhard Industries, Inc., and has the following typical properties: surface area, 30 m^2/g; crystallite size, 100 Å; bulk density (settled), <1 g/cc.

American Cyanamid Type AB-1 electrodes utilize platinum black of this type. In the work reported here, Type AB-1 electrodes have been taken as a standard for comparison of modified structures. A brief discussion of Type AB-1 electrodes together with typical performance data is given in Section 4.1.

4.1 American Cyanamid Type AB-1 Electrodes

Type AB-1 electrodes are formulated to contain 9 mg Pt/cm^2 (electrode area) supported on 100 mesh, 2 mil wire nickel screen. The formulation is such that the electrodes are waterproof, and possess a high degree of porosity. The waterproofing prevents the electrode from becoming flooded with electrolyte and thus permits intimate contact between gas, catalyst and electrolyte. Teflon is used as a binder-waterproofing agent. Porosity in the electrode provides a large exposed catalyst area and aids in gas-liquid contacting. Typical hydrogen-oxygen performance data for standard electrodes are shown in Figure 4-1.

TYPICAL PERFORMANCE OF TYPE AB-1 ELECTRODES

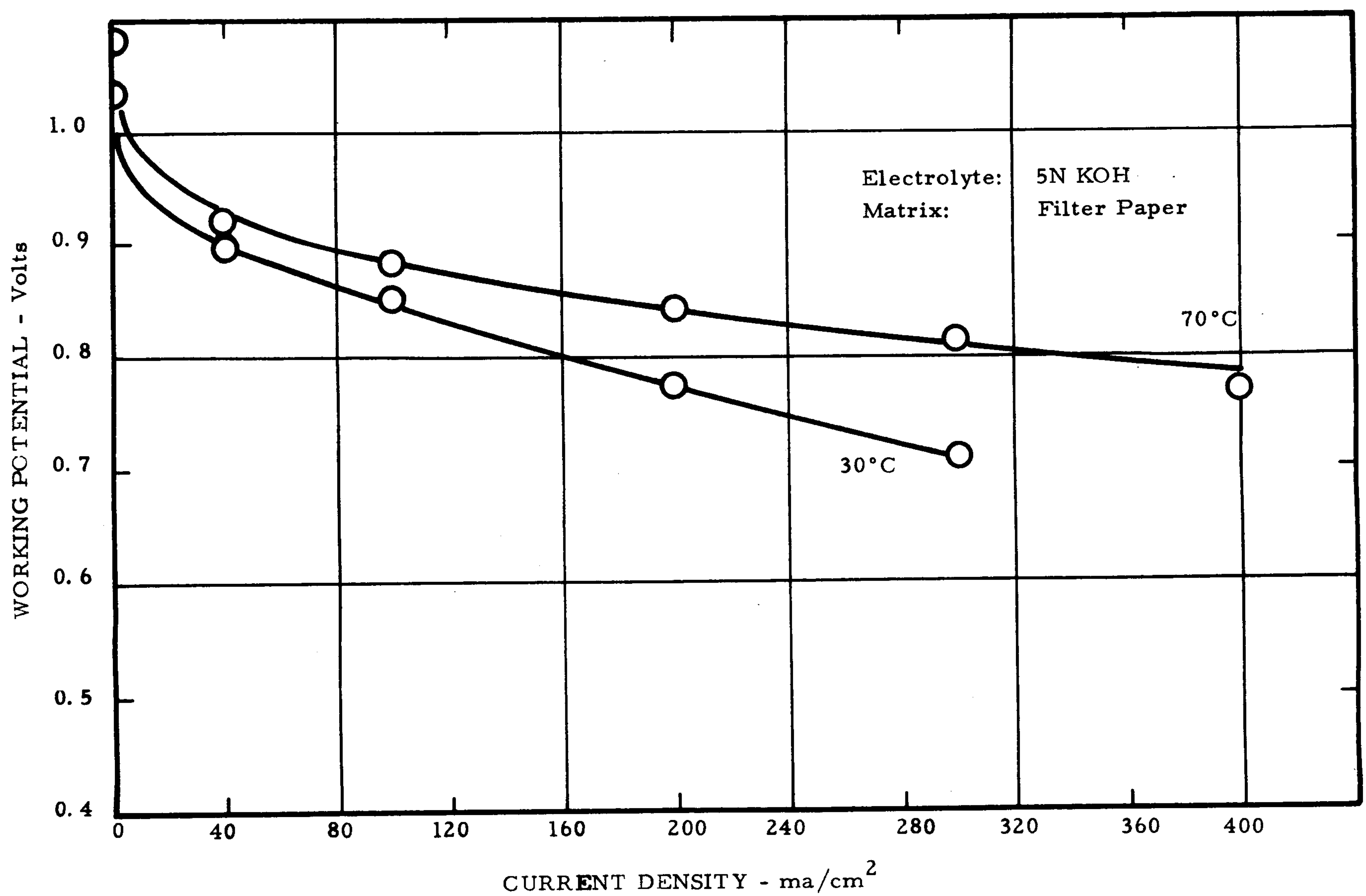

FIGURE 4-1

4.2 Modifications of Type AB-1 Electrode

Table 4-1 shows modifications of the Type AB-1 electrode that were made. The first modification was to increase the standard loading from 9 mg Pt/cm^2 to 20 and 40 mg Pt/cm^2. It was found that in making the higher loading electrodes some difficulties were encountered in bonding catalyst to the support screen. Various support screen structures were tried, therefore, and a "sandwich" structure was developed and found to hold the electrode material satisfactorily. Expanded nickel also appeared to be capable of good electrode-material retention. Expanded nickel may be advantageous also because of the absence of points of high electrical resistance such as may exist where the warp wires contact the weft wires in a screen support.

Several modifications of the basic electrode formulation were also tried. The Teflon level was reduced from 25% to 12.5% to determine the effect of waterproofing level on performance. Finally, the formulation was adjusted to provide a relatively less dense or more open, porous catalyst layer.

4.3 Polarization Data: Modified Electrodes

4.3.1 Test Procedure

Details of the one-inch cell used in evaluating electrodes are given in section 5.2.2. The cell is assembled with discs of the same electrode sample on both the hydrogen and oxygen sides of the cell. The standard matrix material is one thickness of #42 Whatman filter paper.

TABLE 4-1

MODIFICATIONS OF TYPE AB-1 ELECTRODE

Electrode No.	Platinum Loading mg/cm^2	Formulation	Support
S-6609-1-1	20	Standard	70 mesh, 4.5-mil screen
S-6609-1-2	20	Standard	100, 100 mesh "sandwich"
S-6609-3-1	20	Standard	5 Ni 7-4/0 expanded nickel
S-6609-5-1	40	Standard	40 mesh, 10 mil screen
S-6609-4-1	40	Standard	70, 70 mesh "sandwich"
S-6501-47-1	9	Increased Porosity	70 mesh, 4.5-mil screen
S-6609-3-2	20	Increased Porosity	70, 100 mesh "sandwich"
S-6609-3-3	20	Decreased Water proofing	70, 100 mesh "sandwich"

Hydrogen is first passed through both sides of the cell for 2 minutes and then the internal resistance is measured. (A high R_I sometimes indicates improper assembly.) Hydrogen and oxygen (or air) flows are started and the cell temperature is raised to 70°C with the cell heaters. The open circuit voltage is measured and then the external load is increased stepwise every two minutes. Gas flow rates are adjusted to maintain the water balance at each load. When testing with oxygen, inlet hydrogen and oxygen flows are kept equal. With air, a 2:1 ratio of air to hydrogen is used. Voltage across the cell is determined just before and just after the current density is increased to a new level.

4.3.2 Performance with Hydrogen-Oxygen

Polarization curves were obtained on three sets of electrodes cut from each of the modified electrode sheets described in section 4.2. The averaged data for each sheet are listed and compared with averaged data for two standard Type AB-1 electrode sheets in Table 4-2.

Because differences in performance between electrodes appeared to be very small, the data were subjected to statistical analysis in order that more meaningful conclusions could be reached.

In the method used (an outline of which is given in the appendix) it was possible to "pool" the performance data for each electrode sheet and derive a number to express its "performance". This number is designated as $\hat{y}$ (volt) at 200 ma/cm^2. All the $\hat{y}$'s were then used to determine whether significant differences existed between electrodes at the 95% confidence level. From the statistician's point of view, based on the experimental data that were obtained, differences in performance

TABLE 4-2

PERFORMANCE OF MODIFICATIONS OF TYPE AB-1 ELECTRODES

Electrode	S-6609-2-1	LD-213-358-1	S-6609-1-2	S-6609-1-1	S-6609-3-1	S-6609-5-1	S-6609-4-1	S-6501-47-1	S-6609-3-2	S-6609-3-3
Platinum Loading mg/cm^2	9	9	20	20	20	40	40	9	20	20
Formulation	Std	Std	Std	Std	Std	Std	Std	Increased Porosity	Increased Porosity	Decreased Waterproofing
Support Screen	100 Mesh	100 Mesh	100 Mesh "Sandwich"	70 Mesh	5 Ni 7-4/0 Expanded Nickel	40 Mesh	70 Mesh "Sandwich"	70 Mesh	70, 40 Mesh "Sandwich"	70, 100 Mesh "Sandwich"
	Working Voltage at 70°C (Average of Three Tests)									
Current Density ma/cm^2										
0	1.036	1.036	1.036	1.043	1.036	1.047	1.046	1.036	1.040	1.040
40	0.923	0.918	0.934	0.946	0.929	0.944	0.934	0.913	0.927	0.938
100	0.884	0.882	0.899	0.908	0.895	0.907	0.900	0.875	0.892	0.902
200	0.844	0.836	0.848	0.866	0.847	0.870	0.859	0.840	0.848	0.859
300	0.812	0.790	0.799	0.832	0.820	0.846	0.825	0.808	0.813	0.823
400	0.769	0.593	0.771	0.788	0.750	0.799	0.793	0.767	0.749	0.787

could have been due to: (1) variations in test procedure and/or between electrodes from a given sheet, (2) sheet to sheet variation, i.e., inherent variability in the manufacturing technique, and (3) actual differences in the electrode modifications tested. For this evaluation, variation (2) was neglected with the proviso that it will be considered later for further evaluation of the most promising structures indicated by this initial study.

Of the ten electrode sheets evaluated only one (S-6609-3-1, 20 mg Pt/cm^2 on expanded nickel) had too large a "within sheet" error to enable it to be compared on the same basis as the others. The statistical analysis of the remaining nine electrodes is presented in Table 4-3.

The electrodes as arranged in the table, in order of increasing $\hat{y}$, correlate well with loading, the one exception being the 40 mg/cm^2 "sandwich" structure electrode. On the basis of the statistical analysis as summarized in Table 4-3 and subject to the reservations outlined above, the following conclusions may be drawn:

(1) All of the 20 and 40 mg/cm^2 electrodes except the 20 mg/cm^2 "sandwich" structure gave significantly higher performance than either of the two standard electrodes.

(2) Single screen structures at both 20 and 40 mg/cm^2 loadings were significantly better than the sandwich structures.

(3) Increasing the porosity had no significant effect on performance at 9 and 20 mg/cm^2 loadings.

(4) Decreasing the water-proofing level at 20 mg/cm^2 platinum loading gave significantly better performance.

TABLE 4-3

STATISTICAL ANALYSIS OF MODIFIED ELECTRODE PERFORMANCE

Electrode No.	LD-213	6501-47-1	6604-2-1	6609-1-2	6609-3-2	6609-4-1	6609-3-3	6609-1-1	6609-5-1
Pt Loading mg/cm^2	9	9	9	20	20	40	20	20	40
Type	Std. AB-1 Production Sample	Increased Porosity, Single Screen	Std AB-1	"Sandwich"	Increased Porosity "Sandwich"	"Sandwich"	Low Waterproof "Sandwich"	Single Screen	Single Screen
$\hat{y}$ (volt) at 200 ma/cm^2	0.8362	0.8412	0.8452	0.8493	0.8513	0.8616	0.8618	0.8686	0.8748

Note: Any two electrodes not underlined by the same line can be considered significantly different at the 95% level.

Any two electrodes underlined by the same line cannot be considered significantly different at the 95% level.

The 20 mg/cm^2 electrode on expanded nickel screen S-6609-3-1 had a $\hat{y}$ of 0.8543. Statistically, it can be considered different only from the electrodes having the lowest and the two highest $\hat{y}$ values in Table 4-3.

On the basis of the work reported here, it would appear that an electrode with 40 mg Pt/cm^2 and 10-15% Teflon binder on a single 40 mesh nickel screen would be expected to give superior performance. This type of electrode will be prepared and studied in more detail.

Further, since there appears to be a significant initial performance advantage in certain electrodes having higher platinum loadings, several of these will be studied in the life testing program.

4.3.3 Performance with Hydrogen-Air

As discussed in section 4.3.2, differences in performance on hydrogen-oxygen between the various electrodes tested was small. To increase the severity of the test and therefore, hopefully, make it more discriminating, several electrodes were tested with air rather than oxygen. It was felt that the effect of differences in electrode structure might be more easily demonstrated with the additional diffusion burden imposed by the nitrogen in the air. Three electrodes were tested with air/H_2 with results as shown in Table 4-4. In all tests performance was lower by 50-70 mv at 200 ma/cm^2 than with oxygen. With air, performance fell off rapidly at a relatively low current density (200-400 ma/cm^2) indicating the existence of a diffusion limiting process. The results in Table 4-4 indicate the 20 mg/cm^2 electrode made by the "sandwich" technique to be inferior in this respect to either of the two single 70 mesh screen electrodes tested.

TABLE 4-4

ELECTRODE PERFORMANCE

AIR/HYDROGEN

Electrode No.	S6501-47-1	S6609-1-2		S6609-1-1		
Pt Loading (mg/cm^2)	9(1)	20(2)		20(3)		
Current Density (ma/cm^2)	Working Voltage at 70°C					
0	1.014	1.015	1.018	1.010	1.018	1.015
40	0.887	0.874	0.897	0.882	0.888	0.883
100	0.852	0.830	0.861	0.850	0.858	0.843
200	0.773	0.728	0.795	0.800	0.812	0.779
300	0.714	-	-	0.764	0.781	0.700
400	-	-	-	0.718	0.736	-

(1) Increased porosity formulation on 70 mesh x 4.5 mil nickel support screen.

(2) Sandwich structure, with two 100 mesh screens.

(3) On 70 - mesh x 4.5 mil nickel screen.

5. TEST CELL DEVELOPMENT

5.1 Theoretical Considerations

5.1.1 Water Balance Calculations

Successful operation of a matrix-type hydrogen-oxygen fuel cell requires that the water formed electrochemically be removed from the system as it is formed. This has been accomplished in the current program by employing excess flow of gases to remove the water by evaporation. The gas flows required to maintain the water balance depend on cell temperature, electrolyte concentration, the humidity of the inlet gases, and the current density at which the cell is operated.

In a life-testing program, it is reasonable to consider for the sake of simplicity the use of dry gases with no recirculation of excess gas to the cell. Under these conditions, the flows required to maintain the water-balance are determined as follows: From stoichiometry, in unit time:

Eq (1) $N_{WP} = 2/3 N_{GC}$, where N_{WP} = mols water produced, and
N_{GC} = mols gas consumed

Assuming the gases leaving the cell are saturated with respect to the concentration of electrolyte in the cell,

Eq (2) $N_{WE} = N_{GE}(P/\pi - P)$, where N_{WE} = mols water in exit gases

N_{GE} = mols dry gas in exit gases

P = Vapor Pressure of H_2O over KOH at cell conditions

π = Total system pressure

At water balance the water in the exit gases is equal to the water produced. Therefore,

$$\text{Eq (3)} \quad 2/3\ N_{GC} = N_{GE}(P/\Pi\text{-}P)$$

Rearranging,

$$\text{Eq (4)} \quad \frac{N_{GE}}{N_{GC}} = V'_E = \frac{2}{3}\left(\frac{\Pi - P}{P}\right),$$ where V'_E is the exit gas flow rate expressed as a ratio to the stoichiometric gas requirements, in any convenient units. It follows that:

$$\text{Eq (5)} \quad V'_I = 1 + \frac{2}{3}\left(\frac{\Pi - P}{P}\right),$$ where V'_I is the total inlet dry gas flow rate expressed as a ratio to the stoichiometric requirement. The stoichiometric flow rate is a function of the total current only, and may be expressed as:

$$\text{Eq (6)} \quad V_o = .01154\ (CD)(A),$$ where V_o is the stoichiometric gas requirement, mls/min, (measured at 27°C), CD = current density, ma/cm^2, and A = area, cm^2.

Figure (5-1) shows the total gas flow requirements, as calculated from equation (5) and vapor pressure data[16], as a function of cell temperature and electrolyte concentration for a system pressure of 1 atmosphere. It is evident from Figure 5-1 that at or near room temperature, the flow rates required to maintain the water balance are very high. At cell temperatures near 100°C, however, required flow rates approach stoichiometric, particularly at KOH concentrations near 5N.

GAS FLOW REQUIRED FOR WATER BALANCE

(DRY GAS FEED)

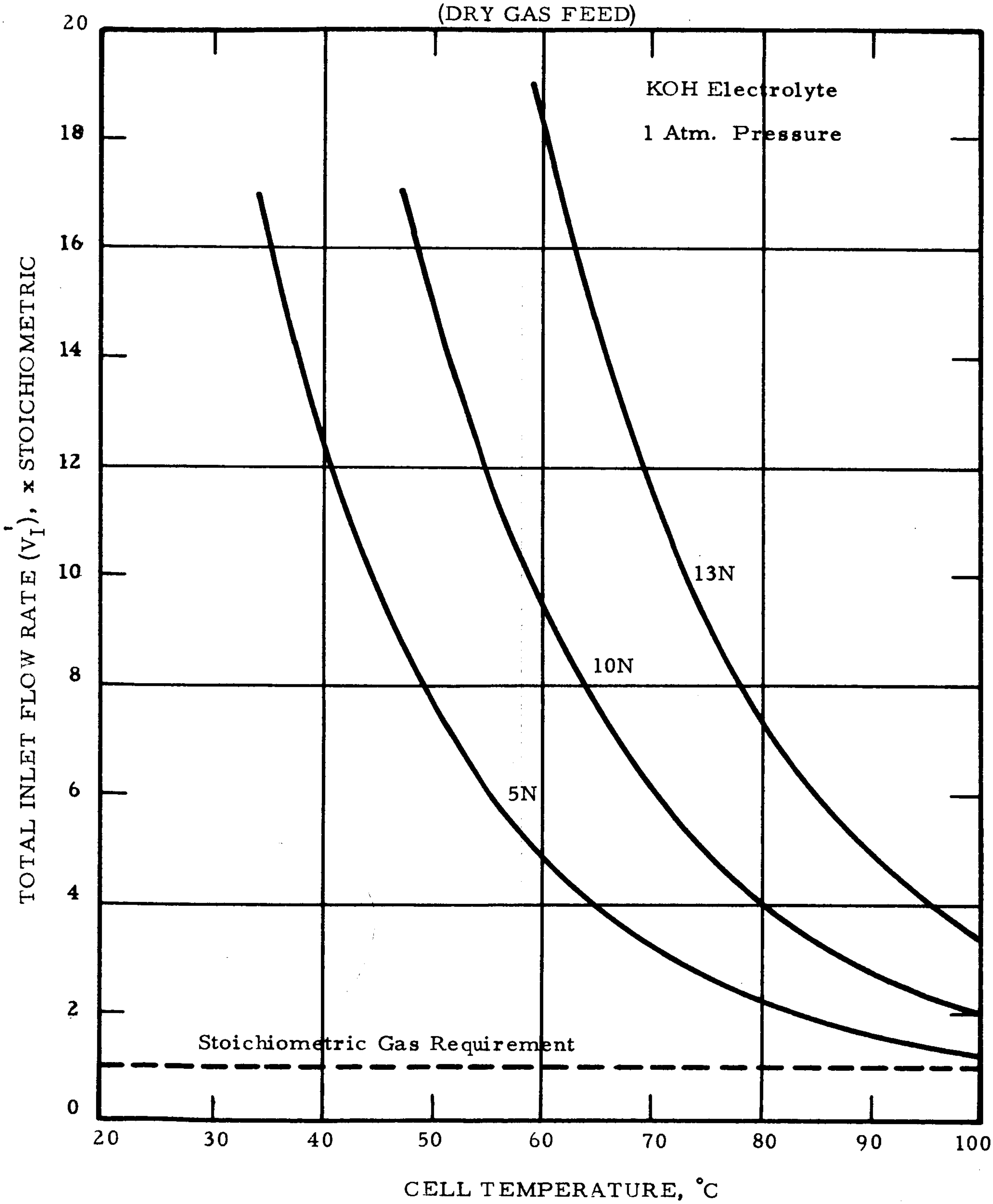

FIGURE 5-1

When dry gases are fed to a cell, there is a large gradient in the driving force for mass transfer of water from the electrolyte phase to the gas phase. Thus there is a tendency for the cell to overdry at the gas inlets even though the overall water balance is maintained. Such localized overdrying may well be detrimental to cell performance. To avoid this, it may be desirable to use gases presaturated with water. By proper selection of the dewpoint of the inlet gases in relation to the cell temperature, it is possible to put a limit on the maximum concentration which can be developed in any part of the cell (so long as the cell temperature is held constant). The electrolyte concentration in the cell cannot exceed that for which the equilibrium partial pressure of water vapor equals the partial pressure of water in the inlet gases. The relationship between cell temperature, dewpoint of the inlet gases, and maximum concentration is given in Figure 5-2. It can be seen that for cell temperatures in the range 70°C to 100°C, the dewpoint of the inlet gases should not be more than 25-28°C below cell temperature in order to ensure that the KOH concentration will not exceed 11N.

For the case in which the inlet gases contain water, an additional term is required in the water balance equation. The water brought in with the inlet gases is given by:

Eq (7) $N_{WI} = (N_{GI}) \left(\frac{P'}{\Pi - P'}\right)$, where N_{GI} is the total mols of dry gas fed and P' is the vapor pressure of water at the dewpoint of the gases

MAXIMUM ELECTROLYTE CONCENTRATIONS WITH PRESATURATED GAS FEED

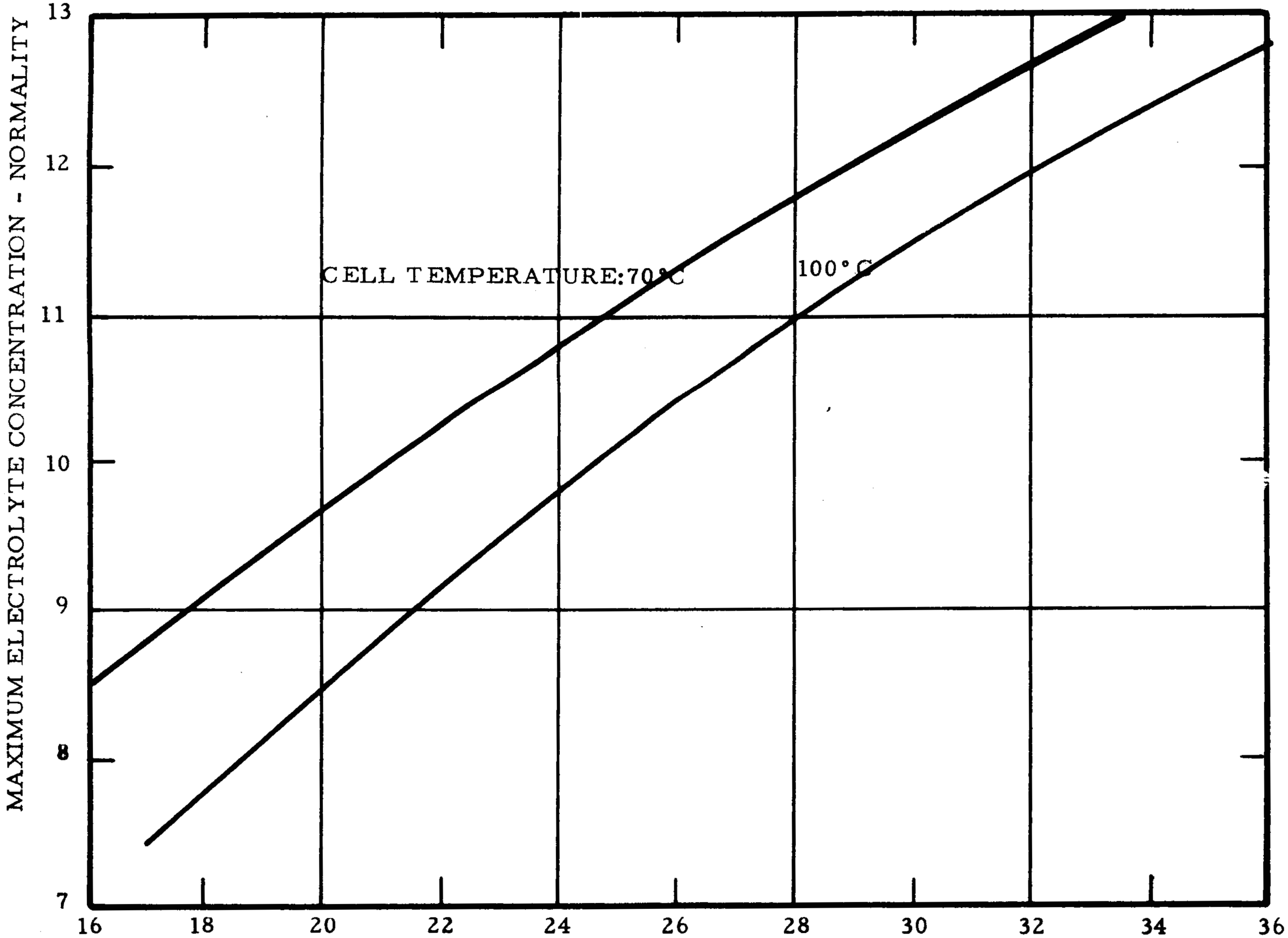

FIGURE 5-2

entering the cell. For a system involving no recirculation of gases, and in which the total inlet flow is passed through a saturator, the dewpoint is the same as the saturator temperature, and the water balance equation becomes:

Eq (8) $$2/3N_{GC} + (N_{GC} + N_{GE}) \left(\frac{P'}{\Pi - P'}\right) = N_{GE} \left(\frac{P}{\Pi - P}\right)$$

This equation may be reduced to:

Eq (9) $$\frac{N_{GE}}{N_{GC}} = V'_E = \frac{2}{3} \left(\frac{\Pi - P}{\Pi}\right) \left(\frac{\Pi + P'/2}{P - P'}\right),$$ from which it follows that

Eq (10) $$V'_I = 1 + \frac{2}{3} \left(\frac{\Pi - P}{\Pi}\right) \left(\frac{\Pi + P'/2}{P - P'}\right)$$

Note that if P' is taken equal to zero, equation (10) reduces to equation (5) for dry gas feed.

Using equation (10) and vapor pressure data for aqueous KOH, the inlet flow rates required to maintain the water balance at various cell temperatures, saturator temperatures, and electrolyte concentrations have been calculated, and are shown in Figure 5-3. Note that when the difference between cell temperature and saturator temperature is less than about 20°C, the required flow rates become quite high, particularly for the lower cell temperatures and higher electrolyte concentrations.

The water balance equation for the case in which the exit gases are recirculated to the cell differs from that which has just been considered.

GAS FLOW REQUIRED FOR WATER BALANCE
(SATURATED GAS FEED)

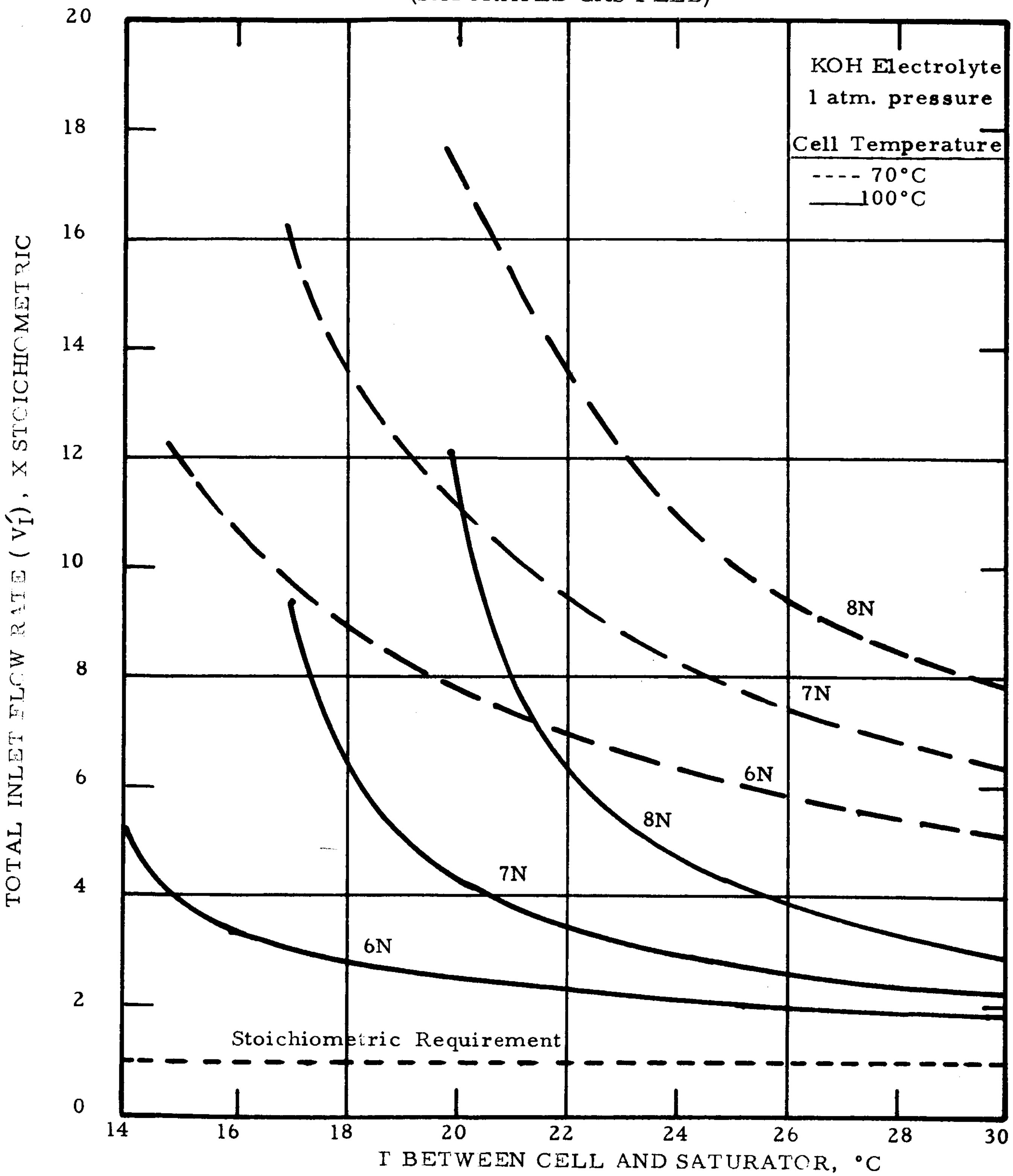

FIGURE 5-3

Assuming that the recirculated gases are passed through a condenser to remove the water electrochemically formed in the cell, the dewpoint of the recirculated gases would be determined by the condenser temperature. The stoichiometric gas requirement would be added as dry gas. For this situation, the water balance equation is:

Eq (11) $2/3\, N_{GC} + N_{GE} \left(\frac{P'}{\Pi - P'}\right) = N_{GE} \left(\frac{P}{\Pi - P}\right)$, where P' is the vapor pressure of water in the recirculated gases. Equation (11) reduces to

Eq (12) $\frac{N_{GE}}{N_{GC}} = V'_R = 2/3 \left(\frac{\Pi - P}{\Pi}\right) \left(\frac{\Pi - P'}{P - P'}\right)$, where

V'_R is the recirculation rate, expressed as a ratio to the stoichiometric gas requirement. The relationship between recirculation rate, cell temperature, condenser temperature, and electrolyte concentration, based on equation (12), is shown in Figure 5-4.

5.1.2 Control of Electrolyte Concentration

The equations presented in Section 5.1.1 provide the basis for determining the conditions for maintaining water balance. For a given initial electrolyte concentration, one can determine combinations of conditions (temperatures and flow rates) to maintain the average concentration in the cell at this level. In principle, the system is self-balancing since any changes which effect the concentration will also change the vapor pressure relationships in such a way as to bring the cell back into water balance at a new average level of concentration. For stable cell operation it is probably necessary to maintain the average electrolyte concentration within fairly narrow limits. (Although good performance can be obtained over a wide range of concentrations, large

GAS FLOW REQUIRED FOR WATER BALANCE
(RECIRCULATED GASES)

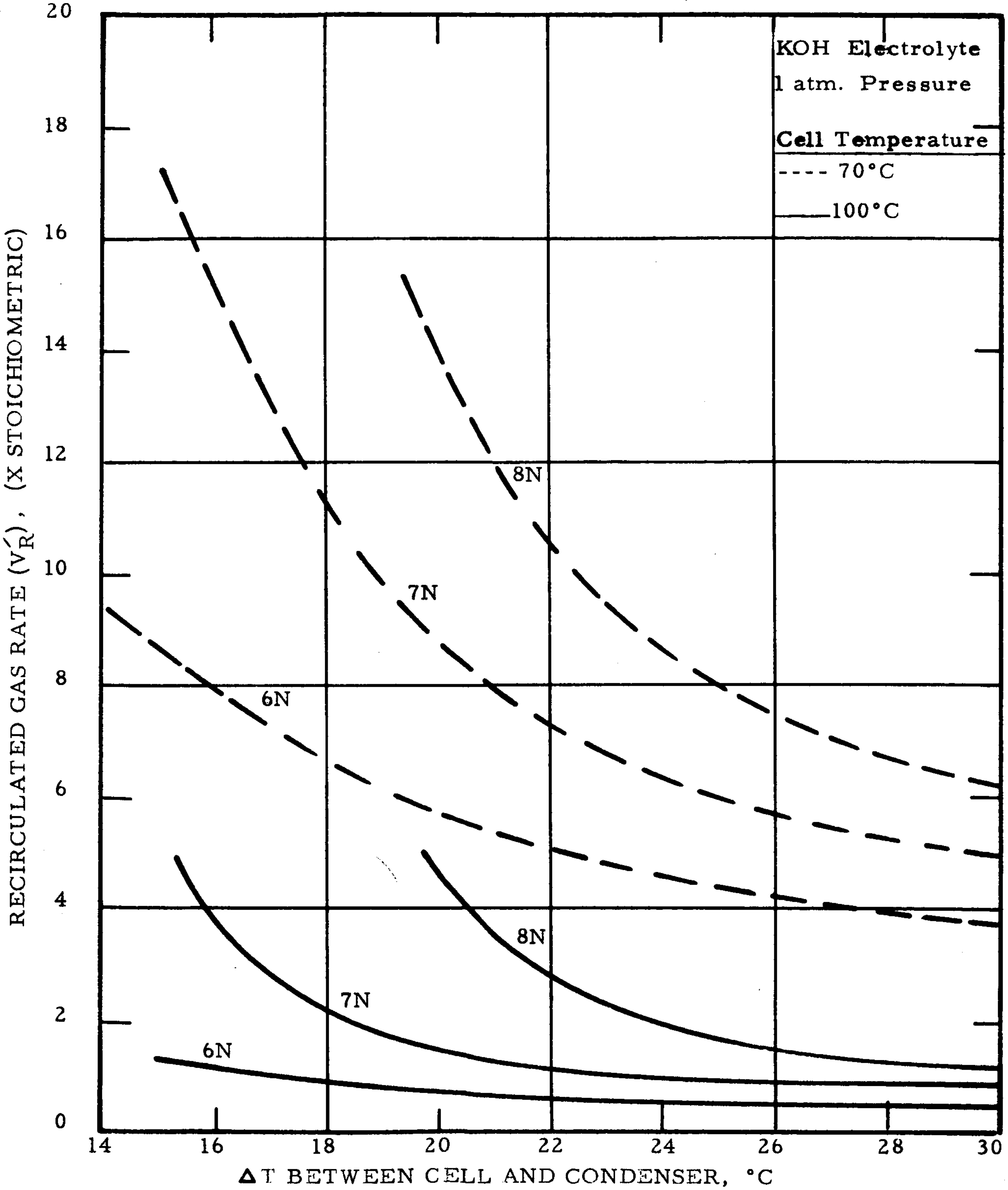

FIGURE 5-4

changes in concentration during cell operation also imply large changes in electrolyte volume, which may be detrimental to performance.)

In order to estimate the degree of control required in a system in which the water balance is maintained by evaporation of water into the gas streams, some sample calculations have been made utilizing the equations presented in Section 5.1.1. Assuming an initial electrolyte concentration of 7N KOH, flow rates to maintain that concentration were calculated for various cell temperatures and saturator temperatures. A control band was then assumed for each controlled variable, as follows:

(1) Cell Temperature: $\pm$ 2°C

(2) Saturator Temperature: $\pm$ 2°C

(3) Flow Rates: $\pm$ 20%

(4) Current Density: $\pm$ 10%

Using the equations in Section 5.1.1, a maximum electrolyte concentration was calculated, assuming for all variables the maximum change within the control band in the direction of drying (i.e., high cell temperature, low saturator temperature, high flows, low current density). Similarly, a minimum electrolyte concentration was calculated assuming that all variable changed in the direction of wetting. The calculated values are summarized in Table 5-1. The calculations show that for operation at cell temperatures of 70-100°C, and with inlet gases saturated at temperatures 20-25°C lower than cell temperature, average electrolyte concentration should not deviate by more than about $\pm$ 1.8N from the original concentration of 7N. With dry gas feed, the range of concentration in the cell for the same degree of control is much greater, particularly at 100°C cell temperature.

TABLE 5-1

CONTROL OF ELECTROLYTE CONCENTRATION

Control Conditions:

Cell Temp.	:	± 2°C
Saturator Temp.	:	± 2°C
Flow Rates	:	± 20%
Current Density	:	± 20%

Initial KOH Concentration: 7N

Cell Temperature:	70°C			100°C		
Saturator Temperature, °C	D.G.(1)	50	45	D.G.(1)	80	75
Control Range, KOH Concentration:						
Max: --	9.5	8.6	8.5	10.2	8.4	8.6
Min: --	3.5	5.2	5.2	2	5.6	5.2

(1) Dry gas feed

The control bands assumed in the above calculations are quite liberal. In life-testing systems, closer control of temperatures and flows is practical, so that it should be possible to control the average electrolyte concentration in the cell to closer limits than indicated in Table 5-1. On the other hand, the calculations deal only with average conditions. It is quite possible that in an actual cell, depending on the distribution of flows, concentration gradients may develop in such a way that local concentrations may fall outside the calculated range.

5.2 Cell Design

Fuel cells of two sizes have been designed and built for the evaluation of electrodes at ambient temperatures and above. Cells having a one-inch circle active area (5 cm^2) were used for obtaining polarization data. For life testing, cells having a 2" x 2" active area (25 cm^2) were constructed. Both sizes utilize electrically heated metal face plates, and are similar in outside dimensions and general configuration. They differ in the size of the active area and in the pattern of gas distribution.

5.2.1 2" x 2" Cell

A typical fuel cell used for life testing is shown in exploded view in Figure 5-5. Significant dimensions of the face plates are given in Figure 5-6. The face plates serve as housing, gas distributors, and current collectors. The matrix sandwiched between the electrodes and saturated with electrolyte, permits ion transport between electrodes and prevents gas mixing. The spacer screens carry current from the electrodes to the face plates and also ensure adequate contact between the electrodes and the matrix. The gaskets prevent liquid or gas leakage out of the cell.

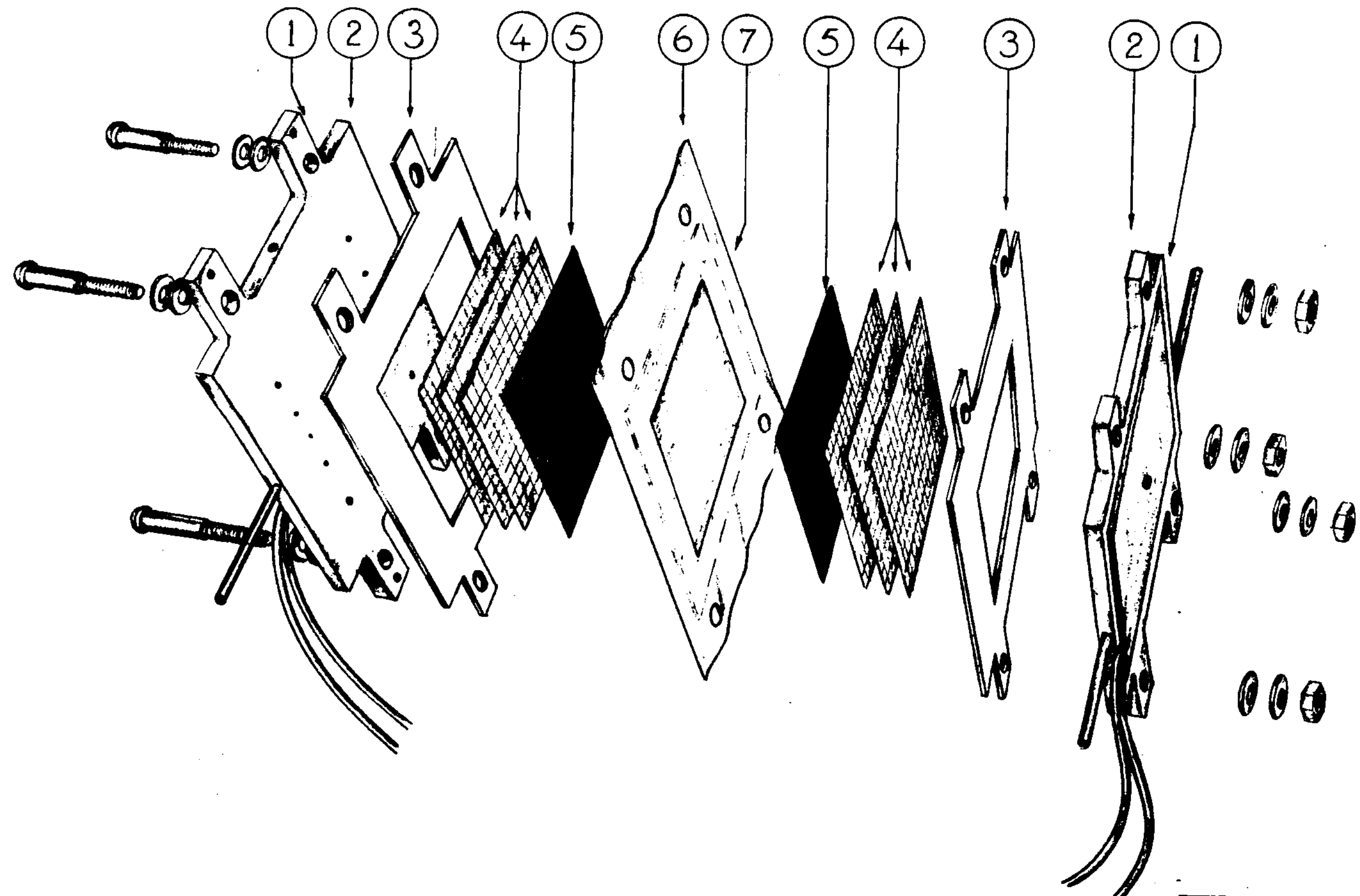

FIGURE 5-5

N°	PARTS DESCRIPTION
1	HEATING ELEMENT
2	FACE PLATE
3	GASKET
4	SPACER SCREENS
5	ELECTRODE
6	MEMBRANE ENVELOPE
7	MEMBRANE

AMERICAN CYANAMID CO.

RESEARCH DEPT.
STAMFORD, CONN.

2"x2" TEST CELL
- EXPLODED VIEW -

DRAWN	DATE	SCALE		
AP		JOB NO.	DWG. NO.	ISSUE
CHECKED	DATE			
APP'V'D				

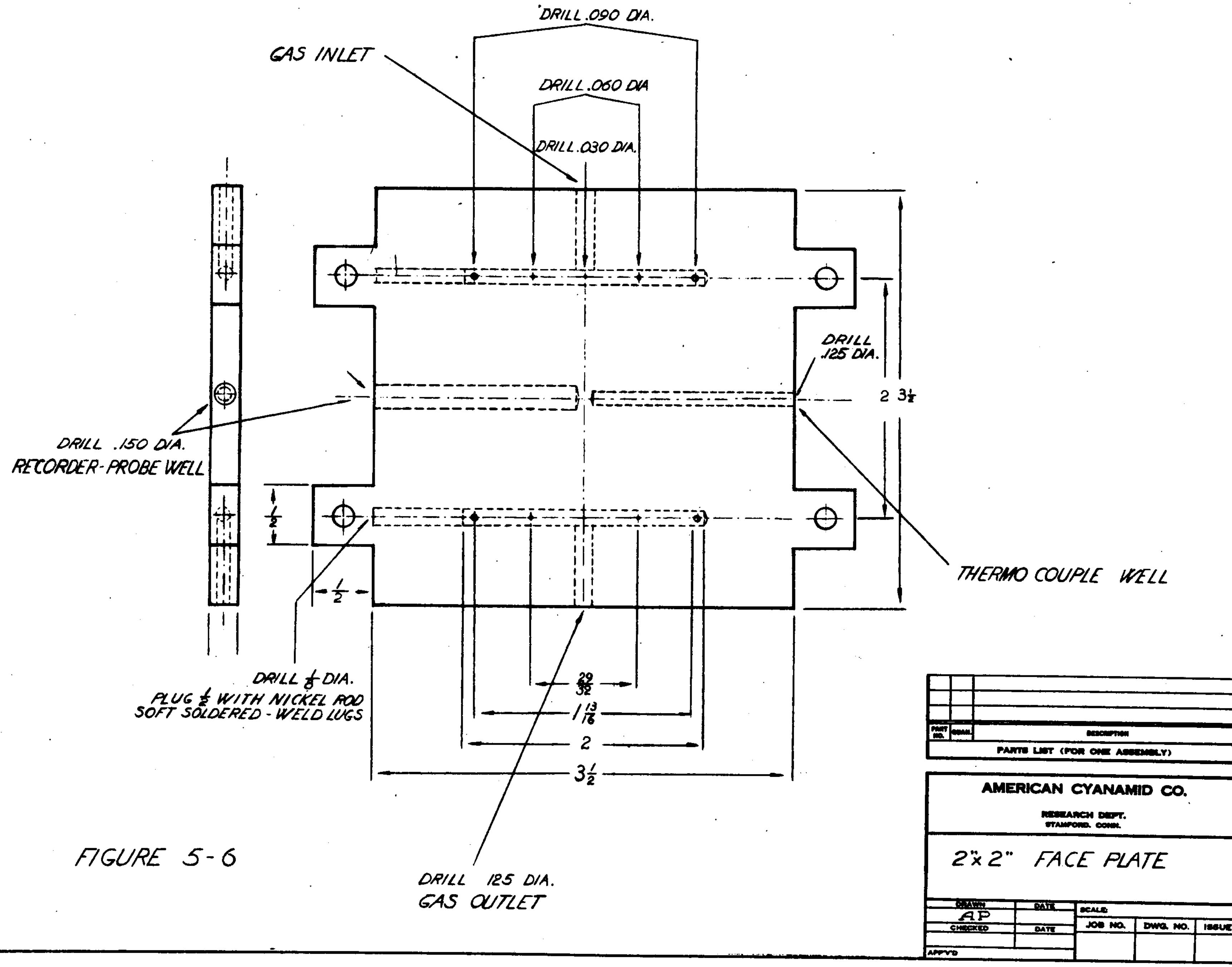

DRILL .090 DIA.
GAS INLET
DRILL .060 DIA
DRILL .030 DIA.
DRILL .125 DIA.
2
3 1/2
DRILL .150 DIA.
RECORDER-PROBE WELL
1/2
1/2
THERMO COUPLE WELL
DRILL 1/8 DIA.
PLUG 1/2 WITH NICKEL ROD
SOFT SOLDERED - WELD LUGS
29/32
1 13/16
2
3 1/2
DRILL .125 DIA.
GAS OUTLET
PART NO.
DESCRIPTION
PARTS LIST (FOR ONE ASSEMBLY)
AMERICAN CYANAMID CO.
RESEARCH DEPT.
STAMFORD, CONN.
2" x 2" FACE PLATE
DRAWN
AP
DATE
CHECKED
DATE
APP'V'D
SCALE
JOB NO.
DWG. NO.
ISSUE

FIGURE 5-6

The face plates are made of nickel (3 1/2" x 3 1/2" x 1/4" thick) with welded lugs made of steel. The inside faces are ground flat. The gas inlet and exit tubes are made of nickel and soft-soldered into the plates. Nickel withstands hot concentrated KOH and conducts current and heat with negligible resistance through the 1/4" thickness used. The gas inlet and exit hole sizes permit gas to flow over the entire width of the electrodes. Bolts for the plates are made of steel. Electrical insulation around the bolts and fiber washers prevent short circuiting. Brass bolts screwed into the lugs serve as electrical contacts.

Gaskets are made either of 50 Durometer silicone rubber (1/16" thick, covered completely with 1-2 layers of Teflon tape 2 1/2 mils thick) or of Teflon sheet (.018 mils thick). The 2" x 2" opening in the gaskets defines the gas compartment of the cell.

The spacer screens are 20, 40 or 80 mesh nickel. On each side of the matrix, the number and thickness of the screens are chosen so that the combined thickness of screens plus electrode equals the gasket thickness to within ± 4 mils. The screens and electrode fit snugly within the gasket opening.

Several different matrix materials have been used. These include:

1. "ACCO" asbestos (20-30 mils thick).
2. Johns Manville Fuel Cell Asbestos Board (34 mils thick).
3. Johns Manville Quinterra Asbestos (10 mils thick).

The characteristics of these materials are described in section 3.2.1. The matrix is the same length and width as the face plate in order to assure a uniform thickness between the plates. To prevent evaporation of water through its edges, the matrix is heat-sealed 1/2" around its periphery in either polyethylene or polypropylene film. Thus, nearly 60% of the matrix surface is not exposed to the gases and serves as a reservoir of electrolyte.

The cells are heated by flat heating elemetns (5 watts/in^2) cemented to the entire outside of the face plates. The cell temperature is regulated to within $\pm$ 0.5°C by an on-off thermistor-type controller and is measured by an iron-constantan thermocouple. The thermocouple and controller probe are inserted from opposite ends of one face plate to within 1/16" of its center. The thermocouple is separated from the gas space by 1/32"-1/16" of plate wall. Measurements at temperatures up to 100°C and at current densities up to 100 ma/cm^2 showed that the temperature of either exit gas at the point where it leaves the matrix is not more than 2°C above the temperature measured by the thermocouple in the face plate.

5.2.2 One-inch Cell

The one-inch cell is similar in general design to the 2" x 2" cell described in section 5.2.1, except that the gasket opening is a 1 1/16" circle to accommodate 1" circular electrodes and spacer screens. A detailed drawing of the face plate is shown in Figure 5-7. In using the one-inch cell, the matrix is usually cut as a 1 1/2" circle. Since this cell is used only for tests of short duration, the silicone rubber gaskets are not protected with Teflon tape, nor are the edges of the matrix sealed with polyethylene film.

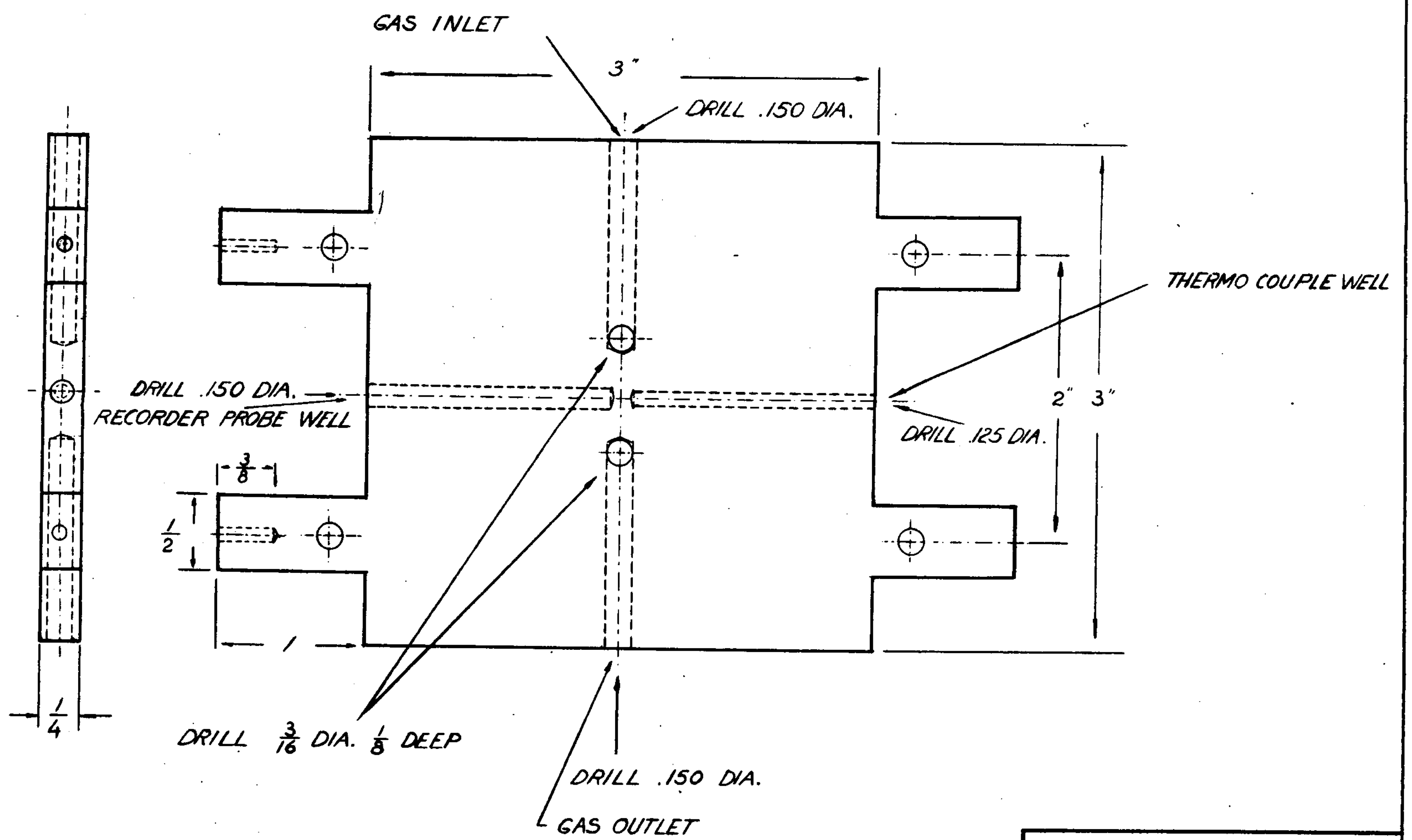

FIGURE 5-7

AMERICAN CYANAMID CO.
RESEARCH DEPT.
STAMFORD, CONN.

1"x 1" FACE PLATE

DRAWN	DATE	SCALE		
AP		JOB NO.	DWG. NO.	ISSUE
CHECKED	DATE			
APP'D				

ISSUE	DATE	BY	DESCRIPTION

REVISIONS

5.3 System Design

The complete life testing system for operation on dry gases, including the cell and all auxiliary equipment is shown in Figure 5-8. Each reactant gas flows from its cylinder through a tube of indicating Drierite (1) and then through a rotameter (2) before entering the cell (3); in runs with carbonate-free KOH a tube of Ascarite (4) is inserted after the inlet Drierite tube to remove traces of CO_2 in the gases. To determine accurately the amount of water removed by each gas stream, drying tubes containing indicating Drierite (5) are connected to the cell by Teflon tubing. The exit gas lines are heated with heating tape (6) to prevent condensation of water before the drying tubes. Rotameters (7) in the exit lines after the drying tubes serve both to detect any gas leakage from the cell and to doublecheck the flow rates. During operation, rotameter floats sometimes become sticky and give false readings and it is desirable not to have to interrupt gas flow even temporarily to clear the inlet rotameters. Current is drawn and measured by the resistor-ammeter (8). Voltage is measured by the potentiometer (9) and continuously recorded (10). The cell is heated by flat heating elements cemented to the outside of the face plate. Cell temperature is controlled by a thermistor-type controller (11) and is measured by a thermocouple (12) and continuously recorded by (13). Internal resistance measurements are made with a Keithley milliohmmeter. A more detailed description of the auxiliary equipment is given in Table 5-2.

TABLE 5-2

AUXILIARY EQUIPMENT

(2,7)	*Rotameters	- Manostat Corp. - #FM 1042B & FM 1043 B predictability flowmeter with Teflon stop and sapphire and stainless steel floats. Total range = 2-400 cc/min for O_2 and 4-1300 cm/min for H_2.
	Cell Heaters	- Electroflex Heat Inc. - Electrothin heating elements 3 1/2 in x 3 1/2 in x 1/32 in thick - 5 watts/in^2 at 115 v.
	Heating Tape	- Scientific Glass H 2100E - 10 ft 480 watts at 115 v. Output controlled by Powerstat.
(8)	Resistor-Ammeter	
	Resistor	- Ohmite (custom made) - dual tapered resistors in tandem (0.5 and 1.0 ohms) permit setting current at 1-10 amps to within 0.5%.
	Ammeter	- Triplet Unimeter
(9)	Potentiometer	- Minneapolis Honeywell - Model #2700 measures voltage to the nearest 0.0001 volt.
(10)	Voltage Recorder	- Rustrak Instruments
(11)	Temperature Controller	- Cole Parmer - #2165 Model RA-thermistor type 0-250°F - Cole Parmer probe #8484-Nylon. Time constant = 3.0 sec. Tip is 1/8" diameter - Controller wired for use with Powerstat.
(13)	Temperature Recorder	- Brown Model No. 153x62P6-x-26 0-200°C 6 points - used with iron - constantan thermocouple having 1/16" diam. bead.
	Milliohmmeter	- Keithley Model 502

*Equipment numbers referred to in text and in Figure 5-8.

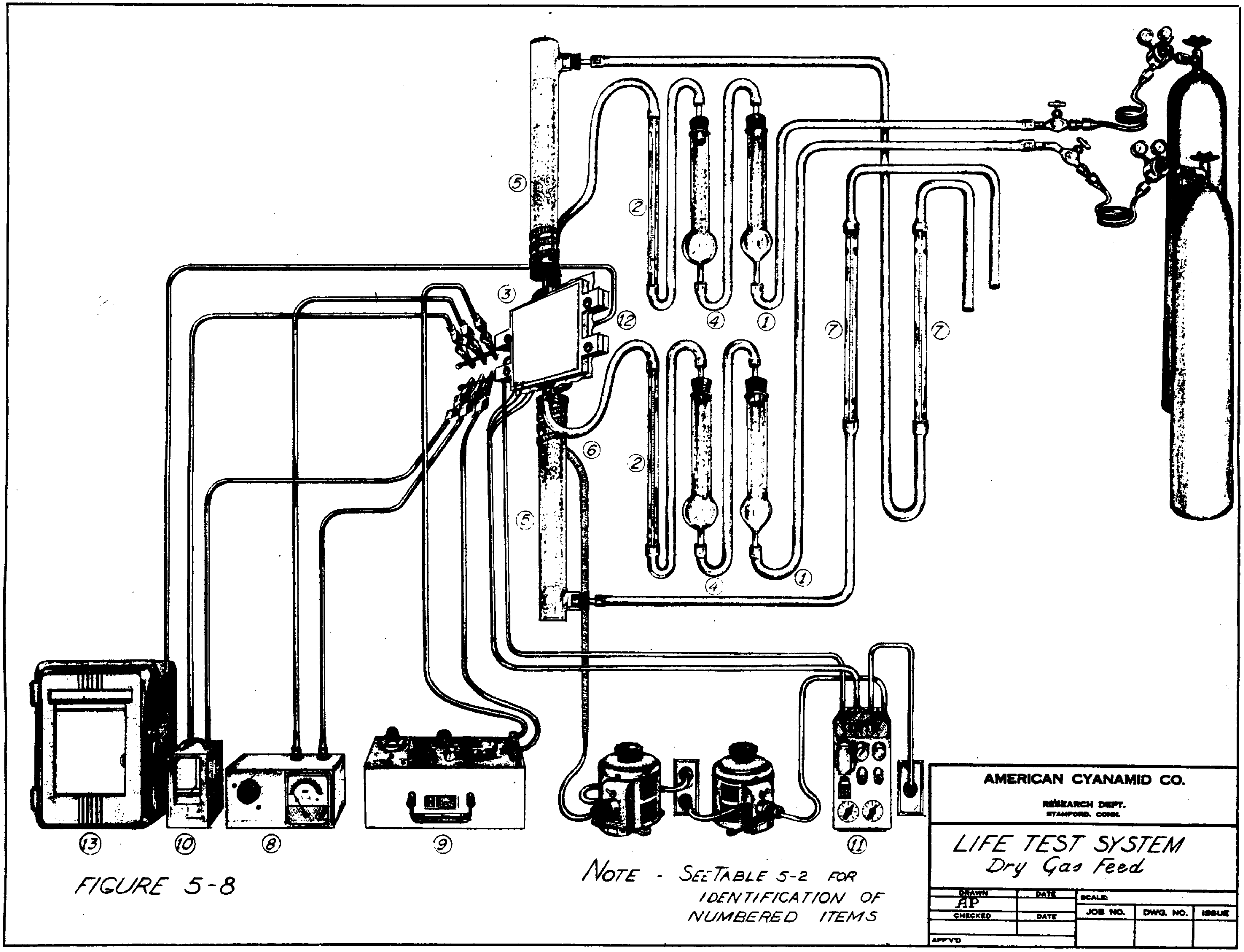

NOTE - SEE TABLE 5-2 FOR IDENTIFICATION OF NUMBERED ITEMS

FIGURE 5-8

5.4 Life-Testing Program

The objective of the life testing program is to operate individual high performance fuel cells for 1000 hours with a minimum drop in cell output (although no actual allowable minimum has been specified). For this work, an equilibrated matrix type cell employing KOH solution as the electrolyte is being used. Stable cell operation requires maintaining the amount of water in the cell constant within certain limits by removing water from the cell at the same rate as it is formed by the cell reaction. Close control of the water balance is necessary to prevent or minimize loss in performance resulting from (1) changes in the average of local concentration of electrolyte, and (2) changes in the quantity of electrolyte solution held in the matrix and electrodes - leading to flooding, or deposition of solid KOH in the electrode pores.

Water removal from the cell is accomplished by evaporation into an excess flow of reactant gas. In principle, it should be possible to run with dry gases on both sides of the cell or with partially saturated gases. Control of water balance for either situation has been discussed in section 5.1. Other possible variations include dead-ending the gas flow on one side or the other. Since it is planned to have as many as 12 test cells operating at one time, it is desirable to operate if possible in a manner which requires the least amount of auxiliary equipment units, the malfunctioning of any one of which could terminate a test. Toward this end, initial life tests have been run with both gases flowing dry.

5.4.1 Cell Output vs. Electrolyte Concentration

Even with very close control of cell temperature, current output and of gas flow rates, the ultimate control of the water balance and of the average electrolyte concentration depends on the inverse relation between the concentration and vapor pressure of the electrolyte solution. Without this inherent control, even a constant water imbalance as low as 1% due to a small deviation in current, temperature, or gas flow rates could cause the cell to become either flooded or dry after several hundred hours of operation. Even with this inherent control, considerable fluctuations in the average electrolyte concentration due to random deviations in the variables affecting the water balance are to be expected (see section 5.1.2). It is important therefore to know how changes in electrolyte concentration affect the voltage at a given current density. Data on the performance of standard Type AB-1 electrodes at 70°C with electrolyte concentrations from 1 to 13N are shown in Figure 5-9. At each KOH concentration, the voltage-current data were obtained over only a 20-30 minute period at gas flow rates set to maintain the water balance so that changes in the average KOH concentration were negligible during the time that the data was obtained. At current densities up to 100 ma/cm^2, the voltage is independent within 15 millivolts of KOH concentration in the range 3-13N. It can be concluded that the average KOH concentration can fluctuate between 3-13N (15-50 wt.%) during a life test without significantly affecting the cell voltage.

PERFORMANCE VS KOH CONCENTRATION

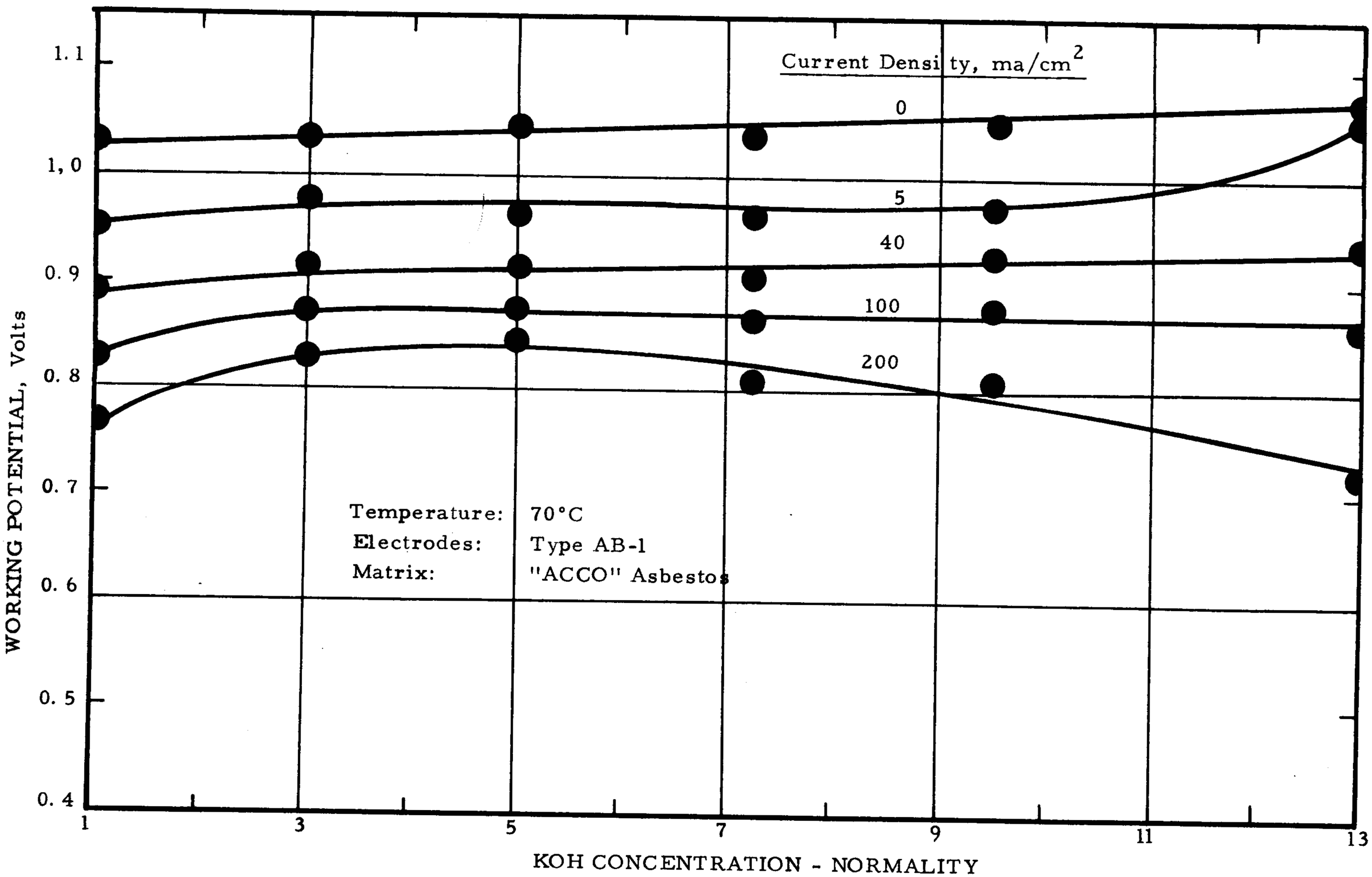

FIGURE 5-9

This conclusion of course makes no assumption covering the effect upon cell voltage of local KOH concentrations which may lie outside the range 3-13N or the effect of the position of the electrode-electrolyte-gas interface, changes in which could result from water imbalance even while the average electrolyte concentration remained in the range 3-13N.

5.4.2 Cell Assembly and Operation

In assembling a 2" x 2" cell for life-testing, the matrix sheet is saturated dropwise with KOH solution, and then hand pressed between two sheets of blotter paper until it contains the proper amount of electrolyte. By experiment it was determined that for "ACCO" asbestos the residual electrolyte loading should be 1.9 times the dry matrix weight. With Fuel Cell Asbestos Board and Quinterra Asbestos, which are denser, a 1:1 ratio gave best results. For most of the work reported here, 5N and 7N KOH solutions were prepared from Baker and Adamson KOH containing 1% (max.) K_2CO_3. In several tests, however, a "carbonate-free" grade solution obtained from the Hartman-Leddon Company was used. This solution contained 15 ppm K_2CO_3 by analysis.

The assembled cell is mounted as shown in Figure 5-8, with the hydrogen inlet at the bottom and the oxygen inlet at the top. In the initial phases of this program, standard grades of hydrogen and oxygen supplied by Air Reduction Sales Company were used. Currently we are using Airco pre-purified grade hydrogen. Typical analyses of these gases, as given by the supplier, are shown in Table 5-3.

TABLE 5-3

TYPICAL ANALYSES OF REACTANT GASES

Gas	Oxygen (Standard)	Hydrogen[1] Standard	Hydrogen[1] Pre-purified
Component		Concentration, ppm	
O_2	Balance	20-200	0.1
N_2	1000-2500	300	210
CO	(2)	(2)	<1
CO_2	5	(2)	3.1
A	1500-3000	(2)	<4
Hydrocarbons	0.2	(2)	1
Dewpoint, °F	-80	-30	-87

(1) Both Standard and Prepurified hydrogen are electrolytic grades supplied by Airco.

(2) Analysis not available.

After purging the inlet lines and heating the exit lines to 110-120°C, the reactant gases are admitted to the cell, and the cell is brought to the desired operating temperature. The temperature controller is set to maintain this temperature, and then polarization data at 0, 40, 100, and 200 ma/cm^2 are obtained. The current density is then set to the desired level (usually 100 ma/cm^2), and the gas flows are adjusted to maintain the water balance during the life test. Throughout the test, cell temperature and output voltage are recorded continuously. Periodic adjustments in load are made as needed to maintain the current density at the initial setting. Cell internal resistance is monitored with a Keithley Model 502 Milliohmmeter. The water removed from the cell in the exit gases is determined by accurate weighing of the drying tubes. The data obtained on water-removal permit estimates to be made of electrolyte concentrations within the cell, and provide a basis for maintaining the overall water balance by making small adjustments in gas flow rates as needed.

5.4.3 Life Tests with Dry Gas Feed

During this phase of the program, emphasis was placed on studying the performance of standard Type AB-1 electrodes. All tests were run at a cell temperature of 70°C, using dry gases. Variations in matrix material, in electrolyte concentration, and in the ratio of hydrogen to oxygen fed to the cells were studied. Principal operating conditions for each life test are summarized in Table 5-4, while typical performance (voltage vs. time) is shown in Figure 5-10.

TABLE 5-4

LIFE TEST SUMMARY

Standard Conditions: Type AB-1 Electrodes
Cell Temperature: 70°C
Dry Gas Feed

Test No.	Matrix (1)	Initial Electrolyte Concentration	Initial Voltage	Current Density ma/cm²	Test Duration (Hrs.)	Remarks
S-6582-4	"ACCO" Asbestos	5.0N	0.877	100	46	See Text
S-6582-8	" "	"	0.875	100	67	See Table 5-5
S-6582-18	" "	"	0.866	100	720	See Fig. 5-10 a
S-6582-40 (2)	" "	"	0.875	100	500	See Fig. 5-10 b
S-6582-56	Fuel Cell Asbestos Board, 30 mils	7.2N	0.856	100	1295	Declined 20 mv in 400 hrs, 120 mv next 400 hrs, 200 mv next 400 hrs.
S-6582-78	Quinterra Asbestos	7.2N	0.834	100	468	Declined 200 mv in 400 hrs.
S-6582-134	Fuel Cell Asbestos Board, 30 mils	5.0N Carbonate-Free	0.830	100	184	Unstable after 100 hrs.
S-6582-150	"ACCO" Asbestos, Two Sheets	5.0N Carbonate Free	0.860	100	502	Declined 150 mv in 400 hrs.
S-6582-86	"ACCO" Asbestos	7.2N	0.845	200	597	Declined 100 mv in 300 hrs.

(1) See Section 3.2 for a description of matrix materials

(2) This and subsequent tests were run on pre-purified hydrogen

LIFE TESTS: CELL OUTPUT VS TIME

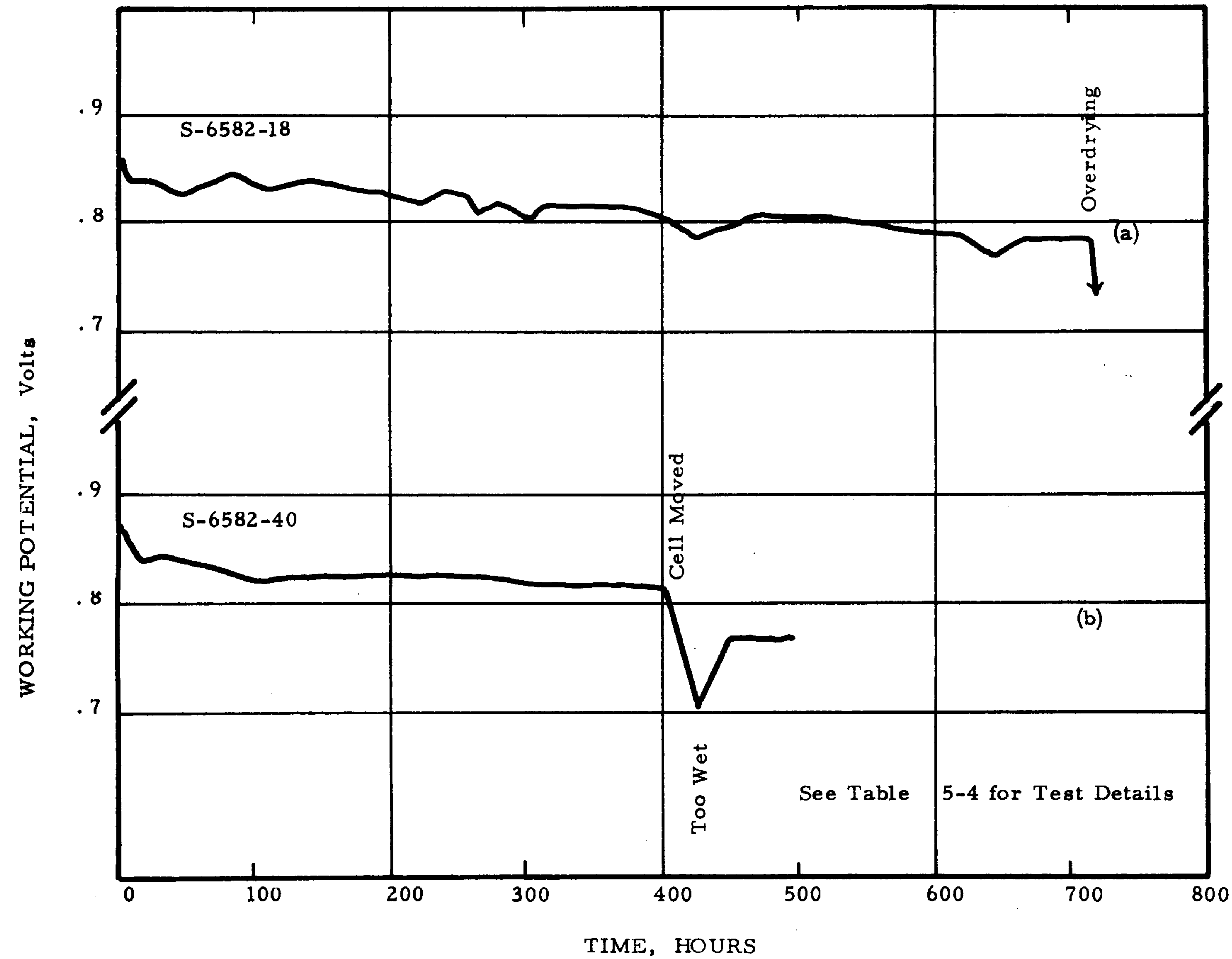

FIGURE 5-10

Water balance calculations, as presented in Section 5.1.1, indicate what the total flow of gases to a cell should be for a given current density, cell temperature, and electrolyte concentration. They do not show how the flow should be divided between hydrogen and oxygen. In the first two life tests, S-6582-4 and S-6582-8, the effect of varying the ratio of hydrogen to oxygen was studied.

Run S-6582-4 was started with a 1:1 ratio of H_2 to O_2 (dry basis) in the exit gases. The voltage dropped 30 millivolts during the first 20 hours. The ratio of H_2 to O_2 was then changed to 1:2, while the total gas flow remained unchanged. During the next 26 hours, the voltage dropped an additional 60 millivolts and the run was terminated. Life test 6582-8 was also started with a 1:1 ratio of H_2 to O_2 in the exit gases. After 24 hours the ratio was changed to 1:2 and after 42 hours to 2:1. The changes in cell voltage and in KOH concentration with time during this test are shown in Table 5-5.

In this table the average KOH concentrations were calculated from overall water balance data, while the estimated concentrations at the H_2 and O_2 exits were calculated on the assumption that each gas leaves the cell saturated with respect to the electrolyte concentration and the end of the matrix adjacent to its exit port. The values shown are representative of 6 to 9 reproducible data points obtained over an 18-24 hour period.

TABLE 5-5

STUDY OF CONCENTRATION GRADIENTS

LIFE TEST 6582-8

Time (Hrs.)	Working Voltage	H_2/O_2 in Exit Gases	H_2O Removed by H_2 / H_2O Removed by O_2	Estimated KOH Conc. at Ends of Membrane (N)		Av. KOH Conc. in Membrane (N)
				H_2 Exit Face	O_2 Exit Face	
0	.875	1.13				
8	.837	1.13	1.62	3.9	7.4	5.0
24	.812	1.13				4.3
25	.808	0.57				4.3
42	.784	0.57	0.52	5.7	5.1	4.0
43	.784					4.0
48	.776	1.86	9.0	1.0	12.2	4.6
67	.805					5.0

During the first 24 hours of test S-6582-8 the voltage fell 63 millivolts despite the fact that the cell was nearly in overall water balance, the total amount of cell water increasing by only 12% and the average concentration of KOH decreasing only from 5.0 to 4.3. During the next 17 hours at 1:2 H_2 to O_2 in the exit gases, the voltage fell, slowly, by 24 millivolts and then rose 21 millivolts during the next 24 hours at a 2:1 H_2 to O_2 ratio.

The water balance data in Table 5-5 reveal the existence of a longitudinal (in the direction of gas flow) KOH concentration gradient whose magnitude depends upon the ratio of H_2 to O_2 in the exit gases. This gradient arises from the relatively greater drying at that end of the matrix which is adjacent to the inlet of the gas flowing at the higher rate. Assuming saturation of exit gases with respect to local concentrations, no overall longitudinal concentration gradient exists when the ratio of water removed by the hydrogen stream to that removed by the oxygen stream equals the ratio of H_2 to O_2 in the exit gases, i.e., both exit gas streams have the same concentration of water. It can be seen in Table 5-5 that the smallest gradient occurred when the exit ratio of H_2 to O_2 was 1:2, and the largest gradient when the H_2 to O_2 ratio was 2:1. In subsequent life tests, therefore, hydrogen and oxygen flow rates were set to give a 1:2 H_2 to O_2 ratio in the exit gases.

Runs 6582-18 and 6582-40 (Figure 5-10) were started and run with a 1:2 H_2 to O_2 exit ratio, with the same matrix material, and at the same KOH concentration and total gas flow as in the two preceding runs. In both runs, following an initial voltage drop of 23-45 millivolts during the first 6-16 hours, the voltage declined by 25-35 millivolts during the next 400 hours of operation. In both runs calculated KOH concentrations were maintained between 4.9 - 5.6 at the O_2 exit and 7.1 - 8.3 at the H_2 exit.

In run 6582-18, switching from standard grade H_2 to prepurified H_2 after 330 hours operation did not produce any change in the slow rate of voltage decline. Over 720 hours of operation, the total drop was 77 millivolts, or 9% of the original voltage. After 720 hours, the cell failed during an overnight period, apparently due to loss of control of the water balance and drying out of the matrix. Following shutdown, the electrodes were soaked in water and a polarization curve was run in the same cell and under the same conditions as at the start of the life test. As shown in Table 5-6, the electrodes have suffered no loss in activity.

TABLE 5-6

ELECTRODE PERFORMANCE AT 70°C BEFORE AND AFTER LIFE TEST 6582-18

Current Density (ma/cm^2)	Working Voltage: At Start of Test	Working Voltage: After 720 Hours
0	1.038	1.023
40	-	0.898
100	0.866	0.864
200	-	0.824

In Run 6582-40, prepurified hydrogen was used from the start. After 400 hour operation, the cell was moved to a new location. Cell voltage then fell overnight from .815 to .703 volts. It was found that the cell temperature was 2°C low, and the total gas flow rate 15% low. Upon restoration of normal conditions, a partial recovery in voltage occurred (to .774 volts) but a complete return to normal output was not achieved and the test was terminated shortly thereafter. These results show the importance of maintaining very close control over operating conditions during life tests with dry gases and indicate that irreversible losses in performance may occur if the cell is out of water balance over an extended period of time. This is particularly so if the cell is drying since with a fixed external resistance a substantial voltage decrease causes a decrease in current and consequently a decrease in the water production rate which accelerates the drying out of the cell.

In life test S-6582-56, 30-mil Fuel Cell Asbestos Board was used as the matrix, and the electrolyte concentration was increased to 7.2N. The lower initial voltage (0.856 volts compared with 0.866 - .877 volts in the preceding tests) reflects the higher cell resistance (14 milliohms compared with 7 milliohms) for the thicker matrix. After an initial drop of 18 millivolts the cell output remained constant to within 10 millivolts over the next 300 hours and then began to decline. The test was continued for a total of 1295 hours. Alternate wetting or drying of the cell by varying the total gas flow, by the use of gases partially saturated with water vapor or by injection of water into the cell did not arrest the downward trend in performance.

The performance obtained with 10-mil thick Quinterra asbestos is indicated in life test S-6582-78. Stable operation in the range .80-.83 v was maintained for 160 hours, but then cell output declined rapidly. Two tests were run with carbonate - free 5N KOH electrolyte, one (S-6582-134) with 30-mil Fuel Cell Asbestos Board matrix, and the other (S-6582-150) with two layers of "ACCO" asbestos. In the first test, stable performance was maintained only for about 100 hours. In the second test, performance declined rather rapidly to .76 volts during the first 68 hours, and then more slowly to about .71 v at 400 hours. In these tests, performance was not better than in earlier tests with electrolyte containing up to about 1% carbonate.

Life test 6582-86 was run to determine whether stable operation could be maintained at a current density of 200 ma/cm^2. After an initial decline of 30 mv performance was relatively stable for about 300 hours. At that point the cell was accidentally short-circuited for a period of two hours, after which the voltage did not again return to a high level.

While there was considerable variation in detail from test to test, the general pattern that emerges from all of the tests reported here shows an initial voltage drop of about 15 to 45 millivolts during the first 24 hours, followed by a period of several hundred hours or more during which the voltage decreases slowly at a rate of about 5-8 millivolts/100 hrs. Finally, there is typically a period of accelerated drop in performance leading to termination of the test. The initial drop occurs even while the average KOH concentration is maintained within $\pm$ 1.0N. The gradual decline following the initial drop occurs even when the longitudinal gradient is limited to not more than 3N.

Examination of the cell components at the end of each test again showed a consistent pattern. Deposits of solid KOH were evident at the inlet ends of the oxygen and hydrogen electrodes, extending in some cases as much as 1/4 inch toward the center of the electrodes. This suggests that gradual build-up of these deposits may have contributed to the deterioration of performance during the test. It should be possible to eliminate the formation of these deposits by operating with the inlet gases partially saturated with water vapor, or by redesign of the cell to provide greater distribution of inlet gas in the longitudinal direction. Both approaches are to be investigated.

5.4.4 Preliminary Work with Partially Saturated Gases

The theoretical calculations of section 5.1 show that partial saturation of the inlet H_2 and O_2 with water vapor can prevent the KOH concentration at any point in the cell from exceeding a maximum whose magnitude depends upon the vapor pressure of the water vapor in the inlet gases. This should prevent the local drying experienced with operation on dry gases. In addition, the gas flow rates can theoretically fluctuate over relatively wide ranges, without causing the electrolyte concentration to fall by more than 2-3N. With these control advantages in mind, work has begun on operation with partially and equally saturated gases.

The saturator design is shown in Figure 5-11. Both saturators are contained in the same constant temperature bath of ethylene glycol. Metered gas is bubbled through a fritted glass sparger disc and then up through 5 1/2 - 7 inches of water before entering the cell. Agitation by the gas keeps the saturator water at the same temperature as the bath.

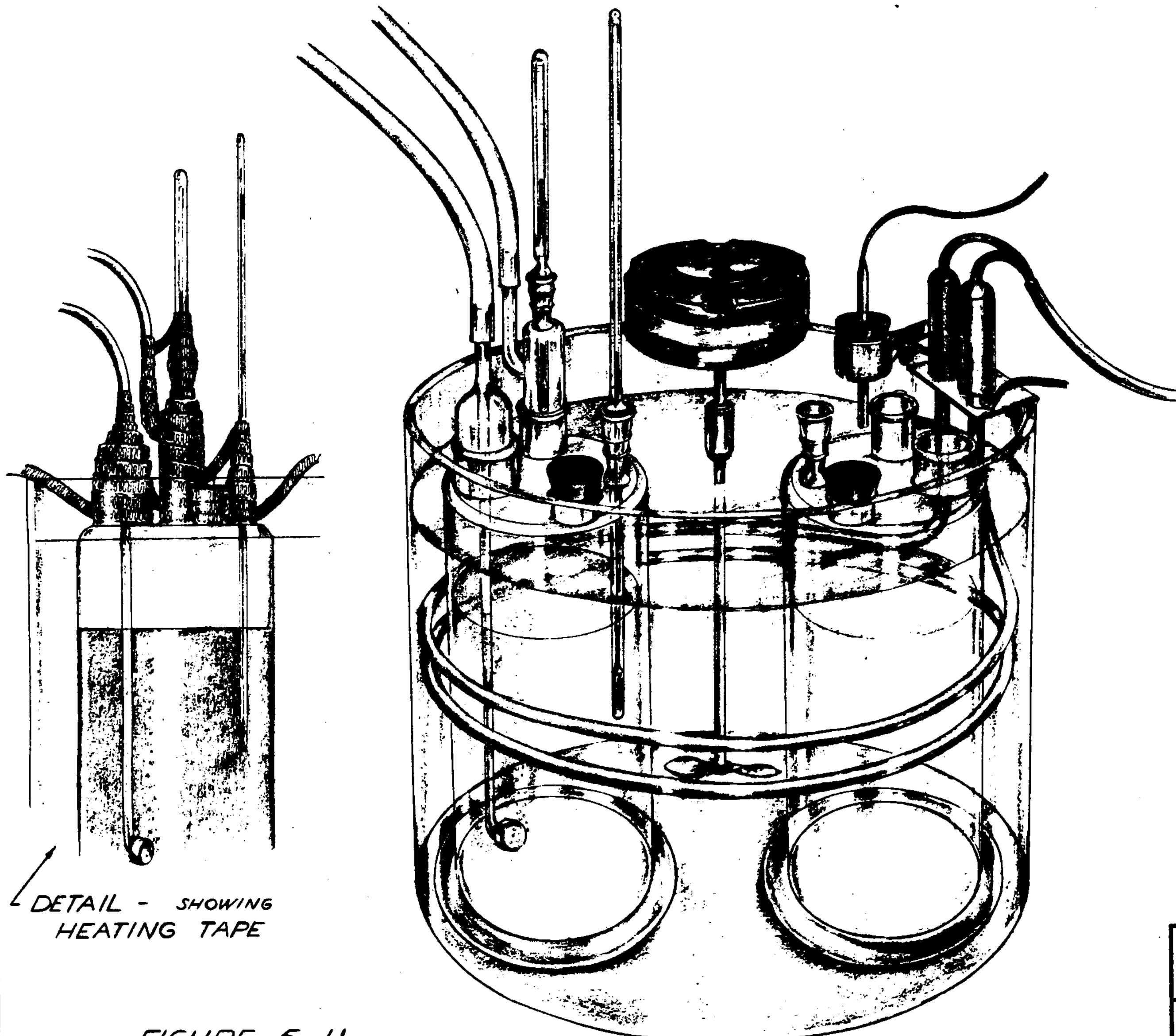

FIGURE 5-11

AMERICAN CYANAMID CO.

RESEARCH DEPT.
STAMFORD, CONN.

GAS SATURATOR
ASSEMBLY

DRAWN	DATE	SCALE		
AP		JOB NO.	DWG. NO.	ISSUE
CHECKED	DATE			
APP'V'D				

ISSUE	DATE	BY	DESCRIPTION
REVISIONS			

Condensation of water vapor on the saturator walls is prevented by having the bath level 2-3 inches above the water level in the saturator. The bath level reaches to the bottom of the glass fittings. Condensation in the fittings and in the lines to the cell is prevented by heating them to 10-25°C above the saturator temperature with heating tape which is wrapped to within 1/4 - 1/2 inch above the bath level. The excess 2-3 inches of bath level, above the saturator liquid level prevents the heating tape from raising the liquid-gas interface temperature above the bulk liquid temperature.

The saturators were tested for saturation of the gases within the range of saturator temperatures 40-90°C and gas flow rates 20-250 cc/min, which would be used to maintain the cell water balance at cell temperatures in the range 70-100°C. In these determinations, the minimum saturator liquid level, 5 1/2 inch, was used. The saturator temperature was measured and controlled to within 0.1°C. Gas flows were measured by rotameters and checked several times during the determination by a water displacement bottle. The water content of the gas leaving the saturators was determined by passing the wet gases through a Drierite tube. In Table 5-7, the percent saturation of the gas is the average of 2-3 measurements made over 10-60 minute intervals. The data show that both H_2 and O_2 leave the saturator essentially completely saturated with water vapor at the saturator temperature. This will permit calculation of the amount of water brought into the cell by each gas during life testing.

TABLE 5-7

SATURATOR TESTS

PERCENT SATURATION OF H_2 AND O_2 LEAVING SATURATOR

Saturator Temp.(°C)	Flow Rate cc/min. at 1 atm & 23°C		Percent Saturation	
	H_2	O_2	H_2	O_2
50	22	26	103	111
	68	76	98	96
	251	252	103	100
91	24	23	97	106
	85	77	102	113
	249	249	97	94

6. FUTURE WORK

The program of work for the next quarter includes investigations in the following areas:

1. Catalysts

Evaluate palladium and palladium/platinum blacks as anode electrocatalysts. Evaluate silver, and silver containing systems as cathode electrocatalysts.

2. Membranes

Evaluate resistivity and performance of asbestos and proprietary membranes at 70°C.

3. Electrode Development

Prepare and evaluate additional modifications of Cyanamid Type A and Type B electrodes including studies of platinum loading, Pt-Rh-carbon electrodes, and graded waterproofing.

4. Life Testing

(a) Develop techniques for life-testing at 100°C, and with saturated gases.

(b) Life test promising experimental electrodes, including:

(1) High Pt loadings
(2) Silver oxygen electrodes
(3) Pt on carbon
(4) Pt-Rh on carbon

(c) Redesign cells for:

(1) Better gas distribution
(2) Testing under pressures to 15 psig

5. Scale-up

Start development of 6" x 6" cells

(a) Preliminary face plate designs and gas distribution studies.

APPENDIX A

STATISTICAL METHODS USED FOR ANALYSIS OF ELECTRODE PERFORMANCE DATA GIVEN IN SECTION 4.3.2

The statistical analysis of the data proceeded as follows: The test values at 100, 200, and 300 ma/cm^2 were used in order to determine the linear relationship between current density and voltage within this range for each of the three sample electrodes taken from each sheet. Least squares estimates of the two coefficients in the straight line fitting the data were obtained for each sample electrode. These estimates were then compared to see if the three slopes and intercepts within a sheet could be considered significantly different. For each sheet an equation was obtained needing either two, four, or six parameters to characterize an electrode type. It was now possible to estimate the variation between electrode samples within sheets. These errors were tested to see if the sample-test error was consistent for all electrode types. This was found to be the case, with the exception of electrode type S-6609-3-1, for which the variability was significantly larger.

The "best" single value to characterize the activity of an electrode type was considered to be the predicted value at 200 ma/cm^2. The least squares (and hence most precise) estimate of this value is given by the means of all nine data points from a given electrode sheet.

In order to say that a <u>real</u> difference exists between electrode types it is necessary to have estimates of the sheet to sheet error (not available from this experiment) as well as the sample-test error within a sheet. However, by using the estimate of the sampel-test error within a sheet, one is able to make some tentative decisions. For example, any differences between electrode types which cannot be considered significant when tested against the electrode sample-test error, would certainly not be significant when tested against the total error. However, any differences which appear significant when tested against the electrode sample-test error, would have to be retested statistically against the sheet to sheet error when it was obtained. This would insure that these differences are simple not manifestations of sheet to sheet variability.

References:

(1) H. C. Brown & C. A. Brown, J. Am. Chem. Soc. 84, 1493 (1962)

(2) H. C. Brown & C. A. Brown, J. Am. Chem. Soc. 84, 1494 (1962)

(3) H. C. Brown & C. A. Brown, J. Am. Chem. Soc. 84, 2827 (1962)

(4a) R. Mozingo, Organic Syntheses Collective Vol. 3, 685

b) R. Adams, et al, Organic Syntheses Collective Vol. 1, 463 (1941)

(5) H. Yao & P. H. Emmett, J. Am. Chem. Soc. 83, 796 (1961)

(6) R. W. Bott et al, Proc. Chem. Soc. 337 (1962)

(7) D. W. McKee, J. Phys. Chem. 67, 841 (1963)

(8) D. W. McKee, J. Phys. Chem. 67, 1336 (1963)

(9) J. G. Aston, J. Phys. Chem. 67, 2042 (1963)

(10) J. G. Aston, private communication

(11) E. S. J. Tomezsko, Thesis Penn. State Univ., Sept., 1962

(12) S. Nishimura, Bull, Chem. Soc. Japan, 34, 1544 (1961)

(13) U. S. Patent 3,056,646

(14) U. S. Patent 3,055,840

(15) Zhur. Neorg. Khim., Vol. 4, p. 2127-2135,(1959)

(16) International Critical Tables, Vol. 3, p. 373

DISTRIBUTION LIST FOR 1st QUARTERLY REPORT

National Aeronautics & Space Administration Washington, D. C. 20546	
Attention: Miss Millie Ruda, Code AFSS-LD	3
Attention: Walter L. Scott, Code RPP	1
Attention: Ernst M. Cohn, Code RPP	1
Attention: George F. Esenwein, Code MSA	1
Attention: H. B. Finger, Code RP	1
Attention: A. M. Andrus, Code FC	1
Attention: J. R. Miles, Code SL	1
Attention: Fred Schulman, Code RN	1
National Aeronautics & Space Administration Goddard Space Flight Center Greenbelt, Maryland	
Attention: Thomas Hennigan	1
National Aeronautics & Space Administration Lewis Research Center 21000 Brookpark Road Cleveland, Ohio 44135	
Attention: B. Lubarsky, MS 86-1	1
Attention: N. D. Sanders, MS 302-1	1
Attention: N. T. Musial, MS 77-1	1
Attention: M. J. Sarri, MS 86-1	1
Attention: R. L. Cummings MS 86-1	1
Attention: H. J. Schwartz, MS 86-1	1
Attention: John E. Dilley, MS 86-1	1
Attention: W. A. Robertson, MS 86-1	1 + 1 repro.
National Aeronautics & Space Administration Marshall Space Flight Center Huntsville, Alabama	
Attention: Philip Youngblood	1
Attention: Eugene Cagle	1
National Aeronautics & Space Administration Manned Space Craft Center Houston 1, Texas	
Attention: W. R. Dusenbury Systems Evaluation & Development Div. Rich Building 6040 Telephone Road	1
Attention: Robert Cohen, Gemini Project Office	1
National Aeronautics & Space Administration Scientific and Technical Information Facility P. O. Box 5700 Bethesda, Maryland	
Attention: NASA Representative	2 + 1 repro.
National Aeronautics & Space Administration Western Operations Office 150 Pico Boulevard Santa Monica, California	
Attention: P. Pomerantz	1
Jet Propulsion Laboratory 4800 Oak Grove Drive Pasadena, California	
Attention: Aiji Uchiyama	1

U. S. Army Engineer R & D Labs
Fort Belvoir, Virginia
Attention: B. C. Almaula, Electrical Power Branch — 1

U. S. Army Electronics R & D Labs
Fort Monmouth, New Jersey
Attention: David Linden, Code SELRA/SL-PS — 1
Attention: Dr. Adolph Fischbach, Code SELRA/SL-PS — 1

U. S. Army R & D Liaison Group (9851 DN)
APO 757
New York, New York
Attention: Chief, Chemistry Branch — 1

U. S. Army Research Office
Physical Sciences Division
3045 Columbia Pike
Arlington, Virginia
Attention: Dr. Sidney J. Magram — 1

Harry Diamond Labs
Room 300, Building 92
Connecticut Avenue & Van Ness Street, N. W.
Washington, D. C.
Attention: Robert Goodrich — 1

Army Material Command
Research Division
AMCRD-RSCM T-7
Washington 25, D. C.
Attention: John W. Crellin — 1

U. S. Army Trecom
Physical Sciences Group
Fort Eustis, Virginia
Attention: Dr. R. L. Echols (SMOFE-PSG) — 1

U. S. Army Research Office
Box CM, Duke Station
Durham, North Carolina
Attention: Dr. Wilhelm Jorgensen — 1

U. S. Army Mobility Command
Research Division
Center Line, Michigan
Attention: O. Renius (AMSMO-RR) — 1

Headquarters, U. S. Army Material Command
Development Division
Washington 25, D. C.
Attention: Marshall D. Aiken (AMCRD-DE-MO-P) — 1

Research Office
R & D Directorate
Army Weapons Command
Rock Island, Illinois
Attention: G. Reinsmith, Chief — 1

Office of Naval Research
Department of the Navy
Washington 25, D. C.
Attention: Dr. Ralph Roberts 1
Attention: Dr. J. C. White 1

Bureau of Naval Weapons
Department of the Navy
Washington 25, D. C.
Attention: Whitwell T. Beatson (Code RAAE-52) 1

Bureau of Ships
Department of the Navy
Washington, D. C.
Attention: Bernard B. Rosenbaum, Code 340 1
Attention: C. F. Viglotti, Code 660 1

Naval Ordnance Laboratory
Department of the Navy
Corona, California
Attention: Mr. W. C. Spindler 1

Naval Ordnance Laboratory
Department of the Navy
Silver Springs, Maryland
Attention: P. B. Cole, Code WB 1

Wright-Patterson AFB
Aeronautical Systems Division
Dayton, Ohio
Attention: R. L. Kerr 1
Attention: J. E. Cooper 1

AF Cambridge Research Lab
Attn. CRZE
L. G. Hanscom Field
Bedford, Massachusetts
Attention: F. X. Doherty 1
Attention: Edward Raskind (Wing F) 1

Rome Air Development Center, ESD
Griffiss AFB, New York
Attention: F. J. Mollura (RASSM) 1

Headquarters, USAF (AFRST-PM)
Washington, D. C.
Attention: Lt. Col. W. G. Alexander 1

Space Systems Division
Attention: SSZAE-11
Air Force Unit Post Office
Los Angeles 45, California
Attention: Captain W. H. Ritchie 1

Air Force Ballistic Missile Division
Attn. WEZYA-21
Air Force Unit Post Office
Los Angeles 45, California
Attention: Captain William Hoover 1

Advanced Research Projects Agency
The Pentagon
Washington, D. C.
Attention: C. F. Yost, Room 3E 153 1
Asst. Director, Material Sciences
Attention: Dr. J. H. Huth Room 3E 157 1

U. S. Atomic Energy Commission
Auxiliary Power Branch (SNAP)
Division of Reactor Development
Washington, D. C. 1

U. S. Atomic Energy Commission
Division of Reactor Development
Advanced Space Reactor Branch
Washington, D. C.
Attention: Lt. Col. J. H. Anderson 1

U. S. Atomic Energy Commission
Army Reactors DRD
Washington, D. C.
Attention: D. B. Hoatson 1

Defense Documentation Center Headquarters
Cameron Station, Building 5
5010 Duke Street
Alexandria 4, Virginia
Attention: TISIA 1

Office DDR&E USW & BSS
The Pentagon
Washington, D. C.
Attention: G. B. Wareham 1

Institute for Defense Analyses
Research and Engineering Support Division
1666 Connecticut Avenue, N. W.
Washington 9, D. C.
Attention: Dr. G. C. Szego 1

Power Information Center
University of Pennsylvania
Moore School Building
200 South 33rd Street
Philadelphia 4, Pennsylvania 1

Office of Technical Services
Department of Commerce
Washington 25, D. C. 20009 1

Alfred University
Alfred, New York
Attention: Proffessor T. J. Gray 1

Allis-Chalmers Manufacturing Company
1100 S. 70th Street
Milwaukee 1, Wisconsin
Attention: Dr. T. G. Kirkland 1

Allison Division of General Motors
Indianapolis 6, Indiana
Attention: Dr. R. E. Henderson 1

American Machine & Foundry
689 Hope Street
Springdale, Connecticut
Attention: Dr. L. H. Shaffer
Research & Development Division 1

Astropower, Incorporated
2968 Randolph Avenue
Costa Mesa, California
Attention: Dr. Carl Berger 1

Battelle Memorial Institute
Columbus 1, Ohio
Attention: Dr. C. L. Faust 1

Bell Telephone Laboratories, Incorporated
Murray Hill, New Jersey
Attention: U. B. Thomas 1

Clevite Corporation
Mechanical Research Division
540 East 105th Street
Cleveland, Ohio
Attention: A. D. Schwope 1

Electrochemica Corporation
1140 O'Brien Drive
Menlo Park, California
Attention: Dr. Morris Eisenberg 1

Electro Optical Systems, Incorporated
300 N. Halstead
Pasadena, California
Attention: E. Findl 1

Engelhard Industries, Incorporated
497 Delancy Street
Newark 5, New Jersey
Attention: Dr. J. G. Cohn 1

Esso Research and Engineering Company
Products Research Division
P. O. Box 215
Linden, New Jersey
Attention: Dr. Carl Heath 1

The Franklin Institute
Philadelphia, Pennsylvania
Attention: Mr. Robert Goodman 1

Fuel Cell Corporation
4300 Goodfellow Boulevard
Building 107
St. Louis 20, Missouri
Attention: Dr. R. A. Cooley 1

General Electric Company
Direct Energy Conversion Operations
Lynn, Massachusetts
Attention: Dr. E. Glazier 1

General Electric Company
Research Laboratory
Schenectady, New York
Attention: Dr. H. Liebhafsky 1

General Motors Corporation
Box T
Santa Barbara, California
Attention: Dr. C. R. Russell 1

Hoffman Electronics Company
Research Laboratory
Santa Barbara, California
Attention: Dr. J. Smatko 1

Leesona Moos Laboratories
Lake Success Park
Community Drive
Great Neck, New York
Attention: Dr. A. Moos 1

McDonnell Aircraft Corporation
P. O. Box 516
St. Louis 66, Missouri
Attention: Project Gemini Office 1

Monsanto Research Corporation
Boston Laboratories
Everett 49, Massachusetts
Attention: Dr. J. O. Smith 1

North American Aviation Company
S & ID Division
Downey, California
Attention: Dr. James Nash 1

Pratt and Whitney Aircraft Division
United Aircraft Corporation
East Hartford 8, Connecticut
Attention: Librarian 1

Radio Corporation of America
Astro Division
Heightstown, New Jersey
Attention: Dr. Seymour Winkler 1

Speer Carbon Company
Research and Development Laboratories
Packard Road at 47th Street
Niagara Falls, New York
Attention: Dr. L. M. Liggett 1

Thiokol Chemical Corporation
Reaction Motors Division
Denville, New Jersey
Attention: Dr. D. J. Mann 1

Thompson Ramo Wooldridge
23555 Euclid Avenue
Cleveland 17, Ohio
Attention: Librarian 1

Union Carbide Corporation
Technical Information Service
P. O. Box 6116
Cleveland, Ohio 44101 1

University of California
Space Science Laboratory
Berkeley 4, California
Attention: Prof. Charles W. Tobias 1

University of Pennsylvania
Electrochemistry Laboratory
Philadelphia 4, Pennsylvania
Attention: John O'M. Bockris 1

Western Reserve University
Cleveland, Ohio
Attention: Prof. Ernest Yeager 1